ADOPTION OF ELECTRIC VEHICLE AND EFFICIENCY IMPROVEMENT OF STORAGE SYSTEM IN ADDIS ABABA

BY

BENYAM GIRMA SIBA

IN PARTIAL FULFILMENT OF THE REQUIREMENTS FOR THE DEGREE OF MASTER OF SCIENCE (MSC) IN CONTROL ENGINEERING

ADDIS ABABA UNIVERSITY INSTITUTE OF TECHNOLOGY

ELECTRICAL & COMPUTER ENGINEERING

20, October 2021

Addis Ababa University School of Graduate Studies

This is to certify that, this thesis is prepared by Benyam Girma, entitled: Adoption of electric vehicle and efficiency improvement of Energy storage system in Addis Ababa and submitted in partial fulfilment of the requirement for the degree Master of Science compiles with regulations of the university and meets the accepted standards with respect to originality and quality.

Signed by the examining committee:

Internal Examiner_____ Signature_____date_____

External Examiner_____Signature_____date_____

Advisor _____Signature_____date_____

Chairman of the School_____Signature _____ date_____

Chair of Department of Graduate Program Coordinator

Declaration

I, the undersigned declare that this thesis is my original work, and has not been presented for a degree in this or any other university, and all sources of materials used for the thesis have been fully acknowledged.

Benyam Girma

Addis Ababa, Ethiopia _____

September 2021 Signature

This thesis has been submitted with my approval as a university advisor.

Advisor's Name

Assistance Professor Mengesha Mamo _____

Signature

Dedication

Dedication to my beloved family for their endless support, encouragement and patience

Preface

The work reported in this thesis was performed at Addis Ababa University, School of Electrical and Computer Engineering as a part of the education to Masters of Science in Industrial Control System Stream. The aim of this thesis is to analyse the impact of geographical landscape, road grad and road dynamics in the process of adoption of electric vehicle in specific case of Addis Ababa/Ethiopia. After analysing the impact, an alternative Engineering solution will be provided using Ultra-capacitors and Batteries.

Acknowledgement

First of all, I would like to thank God for his endless blessings and gifts! I would like to thank my advisor Ass. Professor Mengesha Mamo for his scientific and technical guidance and support throughout this thesis, without his continuous corrections and constructive comments this thesis wouldn't have been successful. I am grateful to all staff of AAIT, School of Electrical and Computer Engineering for giving me the opportunity to create this thesis work and assigning advisor. Especially, I want to express my sincere appreciation and gratitude to Assistances. Professor Dereje Shiferaw and Dr. Lebsewerk Negash for their valuable advice in continuous progress report. I would also like to thank my family, for their endless support, understanding, patience and encouragement in my life. Last but not least, I would like to thank my friends (Yemi, Yemeserach Faris, Danel Abraham and Samuel Alemayehu) for their encouragement and support with valuable ideas. They helped me through the paper evaluation as well as guidance through difficult steps.

Abstract

This thesis contributes to the problem description of the impact of geographical landscape and road dynamics in the process of adoption of electric vehicles in the case of Addis Ababa/Ethiopia. The impact of Addis Ababa road dynamics and topographic distribution of the city have been investigated and it was compared with various international drive cycles like EUDC, NYDC, and WLTP. By considering the worst possible scenario for modelling electric vehicle dynamics and energy storage system; this thesis provides an alternative engineering solution using battery and ultra capacitors. The investigation was done concerning electric vehicle regenerative braking energy gain possibilities and the magnitude of energy consumption from an energy storage system. From the simulation result, it was found that the magnitude of the maximum acceleration-deceleration was about 1.57m/s² and 2.81m/s² respectively and the frequency of stop time was around 31 with in the city. In addition to that, because of rugged nature of the topography; the tractive and regenerative energy consumption of the city was about 6637KJ and -281KJ respectively. It was observed that a larger magnitude of acceleration-deceleration rate and regeneration braking energy has been recorded compared to any other international city. Due to this nature of the city, 8 % state of charge battery variation has been found within 400 seconds of simulation time. From the finding, due to the nature of the city; battery Energy storage system is less efficient when compared to hybrid energy storage system hence electric vehicle implemented in the city of Addis Ababa/Ethiopia need to be redesigned. This thesis recommends fuzzy logic control based battery and ultra capacitor hybrid energy storage system which consider topographic distribution and road dynamics of the city. Adopting electric vehicles without considering the above issue may lead to performing under the manufacturer's specification. Specifically, degradation of batteries and reduced use of the range of travel per single charge.

Keywords: Electric vehicle energy storage, Battery-Ultra capacitor hybrid, Fuzzy logic control, Proportional Integral Control, Geographical distribution, Traffic road dynamics, Drive cycle, Regenerative braking

Contents

List of Figure

List of Table

List of Abbreviations

CRGE	Climate Resilient Green Economy
GTP	growth and transformation plan
DC	Direct Current
SOC	State of charge
SOD	State of Discharge
ESS	Energy Storage System
HESS	Hybrid Energy Storage System
UC	Ultra-capacitor
FLC	Fuzzy logic Control
PI	Proportional Integral
DWT	Discrete wavelet transform
EV	Electric Vehicle
ICE	Internal Combustion Engine
MPC	Model Predictive Control
SPSS	Statistical Package for the Social Sciences
GPS	Global positioning system
Fla	Force of linear acceleration
Fg	Gravitational Force
Frr	Rolling resistance force
Fad	Aerodynamic drag force.
T	Transistor

D	Duty cycle
F	Frequency
V	Velocity of vehicle
RMS	Root Mean Square
M	Mass of vehicle
Fsw	Switching Frequency
CDC	Dc buss capacitance
I	Current
V	Voltage
F	Force
AF	Frontal area
G	Gravitational constant
R	Resistor
L_bat	Battery Inductor
C_bat	Battery Capacitor
D_bat	Battery Diode
I_bat	Battery current
Δ I_bat	pick to pick battery current variation
Δ Vout	Voltage ripple
L_UC	Ultra-capacitor Boost Inductor
C_UC	Ultra-capacitor Boost Capacitor
C_UC_min	Minimum Ultra-Capacitor capacitance
V_UC_max	Maximum Ultra-Capacitor Voltage of converter

V_UC_min	Minimum Ultra-Capacitor Voltage of converter
D_UC	Ultra-capacitor Boost Diode
Vin	Input Voltage
Vout	Output Voltage
ΔI_UC	Ultra-capacitor current variation
Ton	Transistor On
Toff	Transistor Off
VDC	DC buss Voltage
ΔVDC	DC buss Voltage variation
L_UC_B	Ultra-capacitor Inductor buck circuit
C_UC_ B	Ultra-capacitor Capacitor buck circuit
D_UC_ B	Ultra-capacitor Diode buck circuit
I_UC_mean	Mean Ultra-Capacitor Current
I_Bat_mean	Mean Ultra-Capacitor Current
V_UC	Ultra-capacitor Voltage
I_UC_B	Ultra-capacitor current for buck converter
ΔI_UC_B	Ultra-capacitor current variation for buck converter
V_UC_B_max	maximum Ultra-Capacitor Voltage of buck converter
V_UC_B_min	minimum Ultra-Capacitor Voltage of buck converter
V_bat_max	Maximum battery Voltage
V_bat_min	Minimum battery Voltage
C	Capacitor
Etr	Tractive Energy

Ptr	Tractive Power
AASHTO	American Association of State Highway and Transportation Officials
HUDDS	Urban Dynamometer Driving Schedule
NYCC	New York City Cycle
WLTP	Worldwide Harmonized Light Vehicles Test Procedures
NEDC	New European drive cycle
FDRE	Federal democratic republic of Ethiopia
IEEE	Institute of Electrical and Electronics Engineers
WGS	World Geodetic System
PCA	Principal Component Analysis
AM	Ante Meridiem
PM	Post Meridiem
CD	Aerodynamic drag coefficient
Crr	Coefficient of rolling resistance
Mot_power_in	Input power of motor
SOC_BAT	State of Charge of Battery
SOC_UC	State of Charge of Ultra-capacitor
PREF_UC	Reference power of ultra-capacitor
PREF_BAT	Reference power of battery
Ibat_ref	Reference Current of battery
Iuc_ref	Reference Current of ultra-capacitor
IN	Input
OUT	Output

Vbuss	DC bus voltage
PDEM	Demanded power
KW	Kilo Watt
KJ	Kilo joule
W	Watt
N	Newton
PROP_Energy	Population Energy
REGEN_Energy	Regeneration energy
BAT_Energy	Battery Energy
UC_Energy	Ultra capacitor Energy
KVL	Kirchhoff's Voltage Law
MOSFET	Metal Oxide Field Effect Transistor
SOC_bat	State of charge of battery
P_dem	Power demand
P_bat_ref	Battery power reference
nmed	Negative medium
nlow	Negative low
med	Medium
nhigh	Negative high

List of symbols

mΩ	Mili ohm
θ	Teat
m	meter
µf	micro farad
%	percentile
$\frac{d}{dt}$	derivative with respect to time
ρ	air density

Chapter one: Introduction

Air pollution is a major adverse consequence of conventional automobiles that use conventional fossil fuels like Petrol and Diesel. If we look at a place where the population is highly dense; Where traffic condition is extremely congested; The condition even become worse. In the case of Ethiopia, Environmental sustainability has been given due attention in all the past development programs and environmental goals have been set within the GTP, The Climate Resilient Green Economy (CRGE) vision and strategy. The CRGE vision is to see Ethiopia being carbon neutral by 2025 [1]. To achieve this and other similar goals, a specific strategy has been prepared in the transportation sector.

This thesis investigates the impact of geographical distribution and traffic road dynamics in the process of the adoption of electric vehicles in the city of Addis Ababa/Ethiopia. The investigation was done with respect to geographical distribution and road dynamics which is a very good indicator of the possibilities of gaining electrical energies for electric vehicle energy storage systems with respect to regenerative braking events. Additionally, the magnitude of tractive power and energy has been studied and compared to different international city drive cycles. After that, based on the characteristics of the city; The paper provides an alternative design approach that improves the efficiency and range of the electric vehicle.

The unique characteristics of the city are described in two scenarios; First because of the geographical distribution of the city; The possibility of gaining a large amount of electrical energy from regenerative braking has been realized. In addition to that, the acceleration-deceleration frequency of the city is very repetitive compared to like NYCD, EUCD, and NEDS. This leads to a significant amount of current drawn from the energy storage system of electric vehicles and may affect the power quality of the battery pack. Moreover, the large current discharge would also shorten the life span of the battery [2].

To handle this problem, the thesis proposed a battery and ultracapacitor hybrid energy storage system. The system mainly uses the battery as a primary energy storage device and additionally, The ultra-capacitors as an axillary energy storage device. Since regenerative braking events happened within a fraction of time, it is critical for the energy storage system to handle this energy as quickly as possible. Furthermore, to improve the efficiency of the energy storage system, the stored energy should supply as quickly as possible to handle heavy demand due to the uphill movement of the vehicle. This nature of auxiliary devices should prevent the large

current drawn from the battery pack Leeds to reduces the voltage drop of the battery pack and improves lifetime.

Combining two power sources requires some control mechanism; The proposed design implement a fully active bi-directional buck-boost converter in conjunction with fuzzy logic and PI controller. The responsibility of the Fuzzy logic control is used for reference power generation and The PI controllers are responsible to generate a duty cycle that consequently tracks the load current and regulates the DC bus voltage of the converters.

From the finding, this thesis recommends that the adoption of electric vehicles in the city of Addis Ababa/Ethiopia must consider topographic distribution and road dynamics of the city. Besides, battery Energy storage system is less efficient when compared to hybrid energy storage system hence require some unique design approach. Adopting electric vehicles without considering the above issue may lead to performing within the manufacturers' specifications. Specifically degrade the performance of batteries and reduced the total range of travel per single charge.

1.1 Statement of problem

- Electric vehicles are designed based on manufacturer location, altitude, weather condition, and the city's driving cycle. Therefore, Implementing Electric vehicles in a city like Addis Ababa could have a significant influence on the energy storage system. Specifically, this could shorten the reliability of the battery's lifetime, Vehicle ranges per single charge significantly influenced; As well as degrading the performance of the vehicle.
- Battery driven electric vehicle has got a limitation in higher power density [8]. So that a hybrid energy storage system using batteries and super-capacitors could be an alternative solution.
- Gasoline vehicles have a significant effect on the environment and this also has an impact on human health. [1]. On the other hand, the cost of the battery of an Electric vehicle is expensive.

1.2 Objective and Aims

1.2.1 General Objective

- Improving range and efficiency of electric vehicle energy storage system by considering impact of geographical landscape and vehicle road dynamics in case of Addis Ababa/Ethiopia.

1.2.2 Specific objectives

- Identifying the impact of geographical landscape, Vehicle road dynamics, And city road grade for the adoption of electric vehicles in the case of Addis Ababa/Ethiopia.
- Suggesting implementable engineering solutions for those challenges in the city by fusing batteries and super-capacitors.
- Modeling of dynamics an electric vehicle based on the worst possible scenario
    - Modeling of Vehicle dynamics
    - Modeling of Energy Storage System.
    - Power splitting control

1.3 Significance of the study

Previously, there is no studies were found to show the impact of landscape and Geographical location and road dynamics in the process of adoption of electric vehicle in case of Addis Ababa/Ethiopia. Hence, the current study has the importance in

- Adding knowledge on the gap regarding this issue
- Leading to new problems for further investigation; based on the findings of this study;
- Providing policy makers, researchers, institutions with adequate, and reliable data so as to implement feasible and appropriate engineering solutions.
- Signalling and motivating the various stakeholders to take appropriate actions by incorporating the issue in their policies and strategies.

1.4 Contribution of the Thesis

This thesis mainly deals with fusing two different energy storage systems and energy splitting strategies based on the dynamic behavior of the road. Specifically, it emphasizes hybridization of battery and ultra-capacitor-based energy storage systems which will improve the efficiency of energy storage, For the case of adoption of the electric vehicle of Addis Ababa/Ethiopia.

Since the performance and efficiency of the electric vehicle can be influenced by different factors, Like the functional area of the vehicle, Availability of Energy sources at a specific time, And the landscape/geography of the city. Those characteristics have a significant challenge for electric vehicle adoption and should have a mechanism in the proposed system architecture.

Because the highest location of the city is about 3400 meter and the lowest point is about 2200 meter above sea level within the city. Considering limited distance travel, the altitude difference is extremely high. Besides that, Considering the specific scenario, the road angle is about 13% within driving about minimum two-three-minute intervals. On the other hand, the city landscape will also have significant capture energy gain to a storage system in the case of regenerative braking due to the altitude difference if the storage system is designed in that way. As far as this factor is concerned, the efficiency of energy storage can be significantly influenced.

Motivated by the above factors, this thesis mainly focuses on the improvement of the energy storage system by fusing batteries and ultra-capacitor banks for efficiency and range improvement of electric vehicles which will adopt in the city. But fusing one or more devices in energy storage devices needs an energy management controller which will dictate the distribution of energy between them.

Most researchers propose an energy split mechanism between different types of energy storage devices and this will be discussed in the next section. As a result, the majority of the proposed energy storage system consider the US, Europe, and Asia's driving dynamics for the testing purpose. But this approach will have a significant deviation from the real-time behavior of vehicle dynamics deployed in Addis Ababa/Ethiopia. So that the effect of the city landscape with frequent contour should be considered on the design of energy storage systems for electric vehicles in Addis Ababa city.

To implement this idea, this thesis proposes rule-based fuzzy logic intelligent controller that has been proposed and designed for the successful energy splitting between two energy storage devices. A key concept in the development of an energy management system has integrated function for dealing with city drive dynamics (from actual city drive cycle), and SOC of the energy storage system (battery/ultra-capacitor) and then performing energy splitting task based on the load demand throughout the cycle. So that efficiency, range of vehicle, a lifetime of the battery and performance of the energy storage system will be improved.

Chapter Two: Literature Review

2.1 Overview

In the first section of the literature review, the overview of the thesis is presented. Secondly, the concept of multiple energy hybridization and its specific sub-topic is then further discussed. Following that, the current ultra-capacitor technology is discussed with its merit in detail. After that, assessing the present research efforts in fussing ultra-capacitor with different energy storage devices are studied. Aiming to enhance battery system with ultra-capacitor technology in electric vehicle power system architectures, this review emphasis to literature concerning hybridized systems having different energy storage arrangement which consist ultra-capacitors. Then Finally the power electronic interfacing concerns involved in a battery-ultra capacitor and control approach for Power splitting/management methods between two energy storage devices are discussed in detail.

2.2 Multiple Energy Storage Systems in an EV

Combining multiple energy storage systems permits the power of each source to be more efficiently utilized. Fundamentally, this involves combining energy systems having high-energy capacity with systems having high power delivery capabilities. In general, energy storage systems capable of delivering continuous power with minimum reduction in their lifespan have greater energy storage capabilities when compared to pulse power delivering devices.

This synergistic configuration exploits the effective use of energy storage systems whenever necessary by maximizing the storage device's efficiency and operational lifespan. Energy storage systems can be further categorized according to their total energy storage capacity, (energy density) and transient power deliverability (power density), thus it is critical to consider those criteria when we choose storage devices. And of course, it mainly depends on the necessary power demand of the duty.

In the application of electric vehicles, Rapid accelerations and decelerations require peak power to be delivered from and transferred to the energy storage system. For a battery-sourced EV, Supplementing the battery pack with a high-power capacity Source results in reducing high power stresses on the battery. Specifically, the combination has several benefits on enhancing battery performance, Increase the life cycle, Limits temperature raising inside the battery [9] [11].

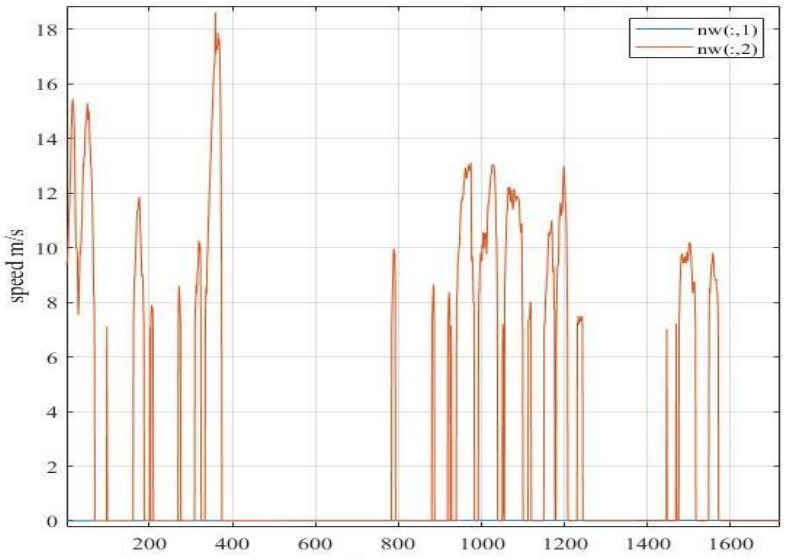

Figure 2. 1 Urban drive cycle of Addis Ababa

If we consider a typical drive cycle of a city, Frequent dynamic behavior requires a short power burst to accelerate the vehicle so this will result in the energy storage system being more stressed to deliver the required power. On the other side during rapid deceleration, kinetically produced energy via regenerative braking, generates currents of high magnitudes. Peak power could be generated during regenerative braking and will be stored via ultra-capacitors. To implement, merging two power sources as a unit require, a control strategy should be mandatory which will dictate the power-sharing strategies between energy storage devices. As a result, fusing multiple energy storage systems in an EV application requires frequent monitoring and administering of the functionalities and the way they share demanded energy.

2.3 The Ultra-capacitor

Ultra-capacitors are electrical energy storage devices typically characterized by higher power density within a specific time interval. Comparing to batteries; they have a much longer cycle-life time than that of electrochemical reaction batteries and usually, their life cycle reaches several million times. Besides that, they are characterized by fast charging and discharging time and a wide operating temperature range. The operating temperature ranges reach from 240˚C to 160˚C. These specific characteristics make Ultra-capacitors a promising candidate for different applications. Among different applications, most researchers believe, UCs are one of the key promising technology enablers for the development of future electric vehicles as well as efficiency improvement of the vehicle. Due to the above fact, Extensive work on ultra-capacitor systems and the associated power and energy management has been carried out worldwide [13-17]. The ultra-capacitors have a high energy density when compared to conventional capacitors. A typical electrolytic capacitor will have a capacitance in the range of tens of Mille-farads. But The same size super-capacitor would have a capacitance of several farads.

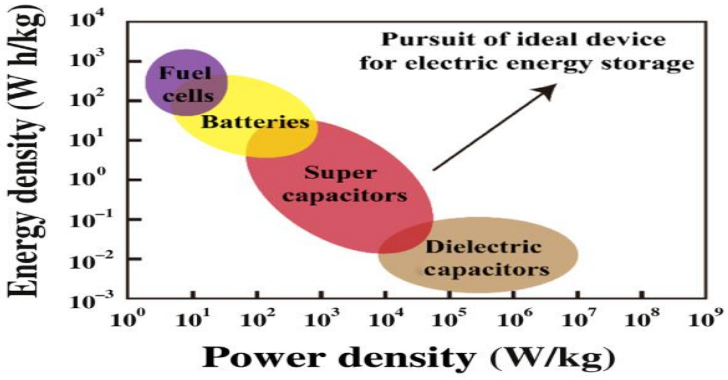

Figure 2. 2 Energy and power densities of typical electrical devices for energy storage [12]

The highest energy density in production now a day is about 30 Wh/kg. Although super capacitors have very high-power density and capacitance values of thousands of Farads are possible, Beside the drawback of energy density capability; The major disadvantage is that cell voltage is limited to about 2.7 V. This is because of the aim to avoid electrolysis of the electrolyte with the resulting emission of gas and deterioration of the super capacitor cell. There are plenty of Ultra-capacitor manufacturer throughout the world. **Table 2.1** shows A listing of current manufacturers of these devices and their respective parameters are shown below.

Manufacturer	Voltage (V)	Capacitance (F)	*ESR* (mΩ)
APowerCap	2.70	55	–
APowerCap	2.70	450	–
Asahi Glass	2.70	1375	2.50
BatScap	2.70	2680	0.20
Fuji	3.80	1800	1.50
Ioxus	2.70	3000	0.45
Ioxus	2.70	2000	0.54
JSR Micro	3.80	1100	1.15
JSR Micro	3.80	2300	0.77
LS Mtron	2.80	3200	0.25
Maxwell	2.70	2885	0.38
Maxwell	2.70	605	0.90
NessCap	2.70	1800	0.55
NessCap	2.70	3640	0.30
NessCap	2.70	3160	0.40
Panasonic	2.30	0.10	0.08
Panasonic	5.50	50	0.08
PowerStor	2.50	2.20	4.57
PowerStor	16.20	65	7.00
Skeleton	3.40	3200	0.47
Skeleton	3.40	850	0.80
VinaTech	2.70	336	3.50
VinaTech	3.00	342	6.60
Yunasko	2.70	510	0.90
Yunasko	2.75	480	0.25
Yunasko	2.75	1275	0.11
Yunasko	2.70	7200	1.40
Yunasko	2.70	5200	1.50

Table 2. 1Commercially available Ultra-capacitor (UC) [18]

2.4 Fusing Batteries and Ultra-capacitors in EV Power system

Although the high capacitance and high-power density characteristics of ultra-capacitors validate its feasibility in electric vehicle applications, the energy capacity limitation dictates the need for a much higher energy sustainable source, in this case, battery bank. The objective of fusing batteries and ultra-capacitors is to take advantage of both devices. Then create an energy storage system with the high energy density features of a battery and the high-power density of an ultra-capacitor. Figure 2.3 shows, the maximum allowable capacity in a proposed energy storage system.

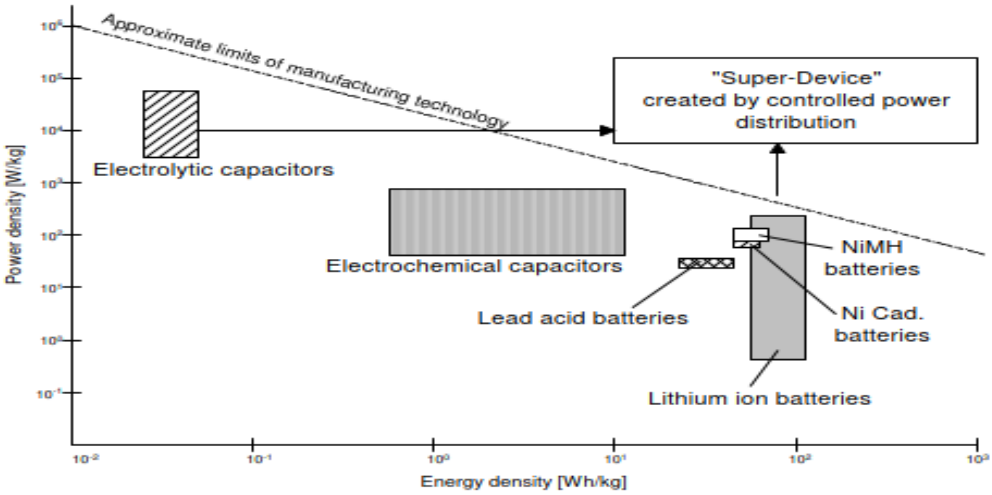

Figure 2. 3 power density vs energy density storage technology [19]

2.5 Topologies of hybrid energy storage

In the essence of combination of energy storage system, the application of semiconductor technology is very significant for the successful implementation of hybridization of energy storage devices. For this reason, high power rated semiconductor devices play an important role in the development of convertor topology specific to the application of electric vehicles. This will allow the energy storage device to be controlled in a safe way. Synchronization of energy storage consisted with ultra-capacitor and battery pack and a bi-directional set up converter plays an important role in this type of application. This type of setup enables the voltage of ultra-capacitor and battery can be buck/boosted in order to meet the required dc buss voltage as well as regenerative mode.

There are different types of convertor topologies and among them directly connected parallel configuration is the most common and simplest configuration of the energy storage is called passive topology [20, 21 & 22].

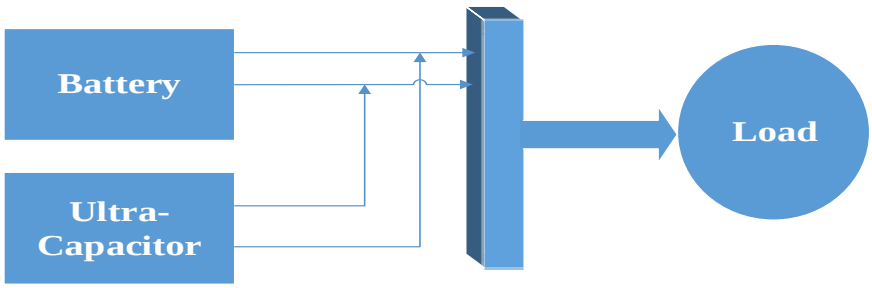

Figure 2. 4 battery and ultra-capacitor direct connection mode

Topology like figure 2.4 is the most common system used for several years and is capable of reducing the magnitude of current drawn from battery [23]. Even though this type of topologies has been used for serval years, it has significant disadvantages on delivery of power to the load. One of them is the uncontrolled power distribution between storage devices.

To enhance the performance of passive topology, semi-active topology has been studied by different researchers and classified the active configuration batteries and ultra-capacitors into two types [24] [25]. The first type has the ultra-capacitor connected directly across the DC bus and the battery connected through a bi-directional DC-DC converter.

In this configuration, Since DC/DC converter is directly connected to the voltage side of the battery, and the battery voltage can be boosted up. So, this will help the battery pack can be made smaller to reduce its weight and volume. Further, with this structure, the battery voltage can be controlled more effectively [29].

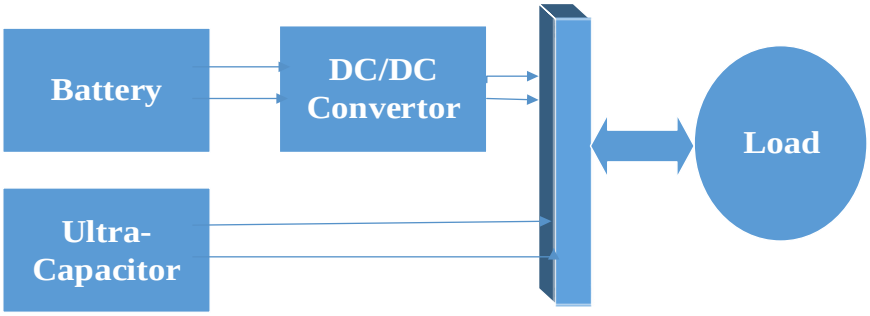

Figure 2. 5 semi active topology with battery power controlled

The second configuration has the ultra-capacitor connected through a bi-directional dc-dc convertor. The voltage of the ultra-capacitor is controlled by a bidirectional DC/DC converter so that the ultra-capacitor can be boosted up to meet the driving power demand. Besides, it can also be implemented for regenerative energy capturing applications [29].

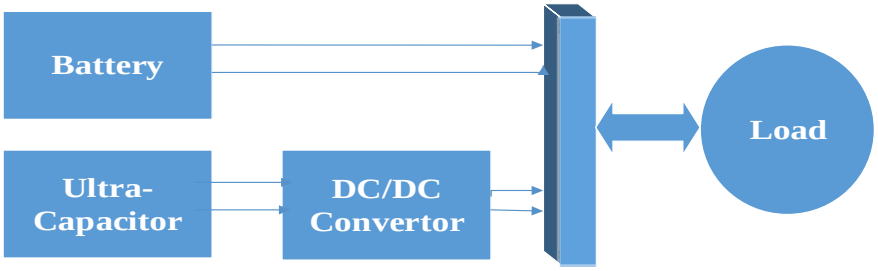

Figure 2. 6 semi active topology with ultra-capacitor power controlled

Different researchers produced comparison data of active and passive power-sharing between ultra-capacitors and batteries under varying load conditions and experimentally verified an increase of power deliverability with the active configuration. They conclude, in the passive system, the power-sharing capabilities of the between devices were dictated by the impedance of the components themselves [26] [27].

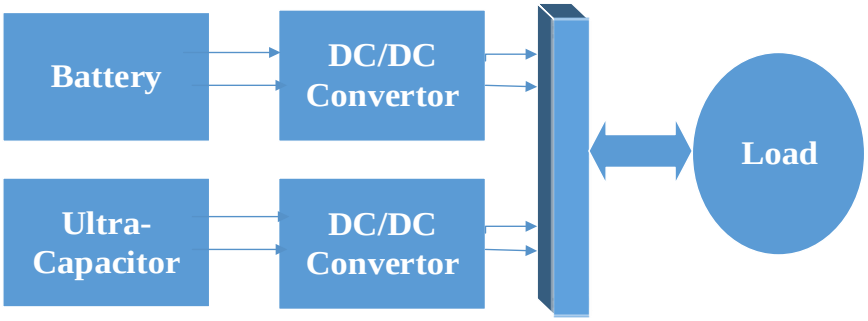

Figure 2. 7 fully active convertor topology

A fully active topological structure is shown in Figure 2.7. In this structure; two bidirectional DC/DC converters are used such that the hybrid power system is decoupled between battery and ultra-capacitor. Therefore, both power sources can be controlled via each DC/DC converter independently. This structure can be more flexible, stable, and efficient for voltage control and power distribution between the battery and the ultra-capacitor. It can also reduce the size and weight of the hybrid energy storage system. The control strategies are much more complicated and the costs of the DC-DC converter devices increased [28].

2.6 Power and Energy Management of battery /ultra-capacitor ESS

The power split between two different types of energy storage systems inside an EV described as follows.

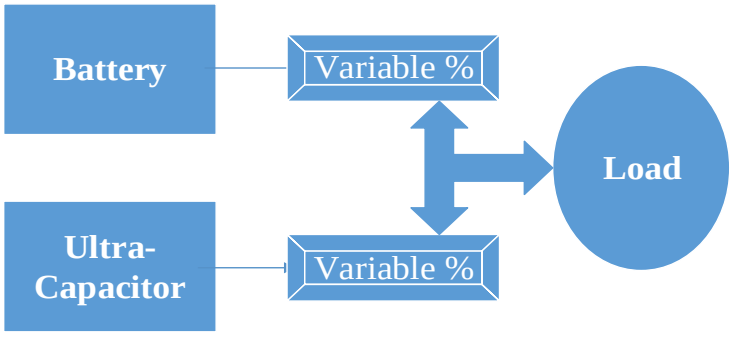

Figure 2. 8 Power and energy split between two sources

The above block diagram of Figure 2.8 shows the contribution of power in different energy storage; specifically, power split between ultra-capacitor and battery bank. Power splitting between two energy sources with different characteristics (energy and power density) needs to implement some control strategies. These control strategies are used to coordinate power flow between different energy storage systems. Since the load behavior highly varies with different factors; The supply power should dynamically be varying as well. To fulfill the load demand and successful operation of the vehicle; The power availability must at least meet the power requirement. This has to be done with further consideration specifically, The SOC of battery and ultra-capacitor must be frequently measured and feed to the controller which is responsible for power split between energy storage systems.

2.7 Control approach for power splitting between energy storage device

So far, several control strategies to manage the above issues have been presented in the literature. In this section, a brief review of existing work will be performed in the area of splitting energy storage between different devices.

Steinmauer and Del Rel [30] proposed to challenge the dual-source power split problem in terms of linear optimal control using known statistical data of vehicle power demand. Their procedure addressed the problem by deriving optimal solutions for a fixed set point, which was then extrapolated to various power demand profiles. They established an optimal power split between a battery and generator. And showed that the battery State of Charge (SOC) was maintained throughout the full drive cycle.

Miller suggested a method to determine power split ratios between batteries, ultra-capacitors, and ICE. In his work, a technique of power spectral decomposition and frequency banding are implemented. The power splits are separated simultaneously in time and frequency by utilizing the discrete wavelet transform (DWT) algorithm. And has adaptive windowing characteristics. Decomposing the power spectrum into designated low, mid, and high-frequency bands correspondingly determine the power splits between the ICE, battery pack, and ultra-capacitors [31].

Lohner and Evers use a voltage reference as the power management control parameter. Their principal method is to regulate the DC link voltage within set point reference voltage. And then using band pass filters and proportional-integral loops to control the current drawn and delivered to several energy storage systems, they have shown the DC-link voltage control method limits

the DC-link voltage rise/fall that occurred because of vehicle acceleration and the voltage rises occur during decelerations [32].

West, Bingham, and Schofield used Model Predictive Control (MPC) method to deal with power split between two energy storage systems used in a pure electric vehicle. They employ MPC with zone control. And they verified that the total energy consumption of an energy storage system in a battery ultra-capacitor system was significantly less compared to a DC-Link voltage control method [33].

A strategy that uses knowledge of subsystem efficiency maps and then computes a reference power split with the Equivalent Consumption Minimization Strategy (ECMS) approach was verified by Guzzella and Sciarretta for sub-optimal but implementable techniques. This is due to the causal control nature of the method. Furthermore, they demonstrated non-causal methods that strongly depend upon the precision of future power profile can lead to an energy management strategy that causes excessive deviation to energy storage system target state of charge [34].

Gielniak and Shen suggested a power split strategy based on game theory. They classified the power sources and the load demands as game players. In their approach, the energy systems are one set of players in a game and adjust its strategy to place itself in a state that produces a high utility. The load demanded power can be seen as the opposing player in a two-player game [35].

Clearly there are numerous approaches to manage multiple energy storage system in a vehicular application system. Variations in approaches shows interesting visions to the problem. This thesis follows a strategy that uses power demand and state of charge HESS as input and then generate a reference power split between battery and ultra capacitor pack using fuzzy logic control.

Chapter Three: Analyses, Modeling and Controller Design

3.1 Materials and Component

The following fundamental components has been used throughout the paper.

- Battery bank
- Ultra-capacitor bank
- Fuzzy logic controller for Energy Control Strategy
- PI controller
- Bi directional (Back/Boost) DC-DC convertors

3.2 Block diagram representation

Figure 3.1 shown below is the proposed block diagram of the hybrid energy storage system. So that based on the energy demand of the drive profile, the available stored energy is delivered to the load using a fuzzy logic controller. The amount of energy storage system available is continuously monitored and controlled.

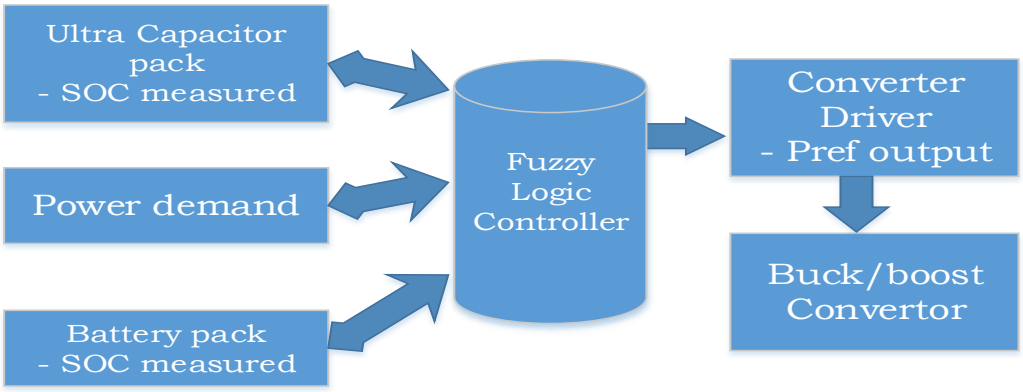

Figure 3. 1 Block diagram of energy storage system

Since the battery pack is the primary energy storage system, it should supply continuous power to the load and the remaining power demand will be handled by the ultra-capacitor. This feature will help the energy storage of the system in a heavy-demand situation. Consequently, in operations that require high power, during hard acceleration or traveling uphill (slope), both battery and super-capacitor supply power to the load. similarly, in operations that require less power, the battery source with characteristics of high specific energy provides power to the DC bus system. In braking and deceleration mode, the regenerative energy will essentially be stored in the source with high specific power characteristics (ultra-capacitor), particularly energy will be stored until supper capacitor become full Stord capacity.

To drive the vehicle safely, the hybrid energy system must be controlled. It's because the overcharging and discharging of the battery and ultra-capacitor build significant problems in the storage system as well as the device itself. By measuring SOC battery and SOC of ultra-capacitor and power demand the necessary control and switching command will be accomplished.

3.3 Drive cycle development

3.3.1 Overview cycle development

A driving cycle is a standardized driving pattern, described by a serious of speed versus timetable [41]. It consists of a sequence of several vehicle operating parameters namely acceleration, deceleration, idle, and cruise condition. These driving parameters are considered representative to specific region [37], [38]. Once we have constructed the drive cycle, and identify the drive parameters; it can be further used for performance comparison of the electric vehicle. Globally there are various standardized drive cycle like European drive cycle, Japanese drive cycle, and US drive cycle. the cycle has been developed considering the road dynamics of the respective countries and it may not be applicable for other cities unless the driving characteristics are similar. This thesis developed a more reflective real time; a non-legislative; transient types is used for the case of Addis Ababa [36].

3.3.2 Selection of study area

In the city of Addis Ababa, there is a lot of road intersection; among them the intersection located in Mesekel square is one of the biggest traffic volume share. It has a wider road diameter and is capable of delivering a large amount of vehicle density.

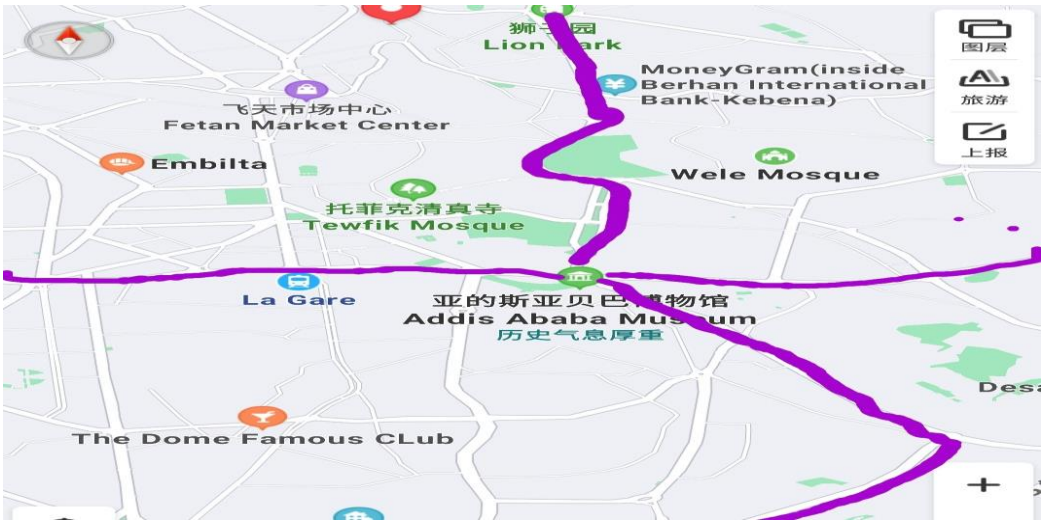

Figure 3. 2 Primary data collected area

As shown in figure 3.2 above, there were four main tributaries that jointed in mesekel square. Because of it was very convenient to construct and identify the real representative of the city. Therefore, this intersection has been selected for the drive cycle development of Addis Ababa city and the four route shown in the table 3.1 below.

Table 3. 1 Geographical position of selected route

Description	Position in rectangular coordinates				
	Altitude	Latitude		Longitude	
	Start to end	Staring	Ending	Staring	Ending
Thorhailoch to Sidst kilo	2326 - 2489	9.0049030	9.0407524	38.7314235	38.7548241
Thorhailoch to Bole	2326 - 2311	9.0050055	8.9825572	38.7200746	38.7653003
Bole to Sidest kilo	2302 - 2489	8.9828197	9.0405372	38.7654679	38.7515226
Sidest kilo to Megenagna	2489 - 2358	9.0407165	9.0098727	38.7536181	38.7805591

3.3.3 Data collection phase

The second step for the development of the city drive cycle is the data collection phase; which was a process of collecting data that effectively represent the behaviour of road dynamics. For the data collection technique; This thesis developed a more reflective real time; a non-legislative; transient types have been adopted throughout the process. And data has been collected by driving dedicated cars on the selected routes in the city.

Since the result the data is strongly correlated to the traffic condition; the pick and off pick hours selected based on prior knowledge of the researcher. And additionally, to get realistic and precise data; the thesis adopted a one second sampling time. Throughout the data collection process; the thesis has been considered that, the pick hours are between at 2:00 to 3:30 and in the afternoon 9:30 to 12:00 in local time. The off-pick hour is the time between 4:00 to 8:30 local time and additionally, the weekend data collection time has been randomly selected.

Generally, the data collection contains 20 datasets and it was collected on selected routes. And each trip has been repeated four different times. Among 20 data set, 16 datasets were collected in a typical urban road dynamic while additional 4 samples were collected on the selected highway roads in the city. The data collection process took approximately three weeks. And the measurement parameters like the speed of vehicles, the time taken, the distance travelled, and the coordinate data has been used by the help of Global Positioning System (GPS) device and third party data logger software application.

Table 3. 2 Sample online data collected

Time	Duration	Speed(km/h)	Distance(km)	Altitude(m)	Latitude(WGS84)	Longitude(WGS84)
2020-12-08 12:40:53	00:00:00	3.168	0.0	2328.0	8.982819727722452	38.76546793579591
2020-12-08 12:40:56	00:00:03	0.0	0.00586531	2333.0	8.982769216475177	38.765483220645436
2020-12-08 12:40:57	00:00:04	0.0	0.00586531	2333.0	8.982769216475177	38.765483220645436
2020-12-08 12:40:58	00:00:05	0.0	0.00586531	2334.0	8.98279395634883	38.765452699402466
2020-12-08 12:40:59	00:00:06	1.944	0.0068581444	2331.0	8.982792036324627	38.76544507422677
2020-12-08 12:41:00	00:00:07	0.0	0.007911926	2329.0	8.982782500987058	38.765445080281324
2020-12-08 12:41:01	00:00:08	0.0	0.007911926	2327.0	8.982781553929422	38.76544889408062
2020-12-08 12:41:02	00:00:09	1.224	0.008809156	2324.0	8.982785381030302	38.765456518044424
2020-12-08 12:41:03	00:00:10	0.0	0.0110173	2316.0	8.982772057541473	38.76547177927365
2020-12-08 12:41:04	00:00:11	0.0	0.0110173	2315.0	8.982772057541473	38.76547177927365
2020-12-08 12:41:05	00:00:12	1.0439999	0.012056042	2315.0	8.982772991580022	38.765460339102106
2020-12-08 12:41:06	00:00:13	0.828	0.0131200375	2314.0	8.98276725740191	38.7654527163478
2020-12-08 12:41:07	00:00:14	0.0	0.015038999	2311.0	8.982760608631159	38.76546797334126
2020-12-08 12:41:08	00:00:15	0.0	0.015038999	2311.0	8.982759661600053	38.7654717871335
2020-12-08 12:41:09	00:00:16	0.0	0.015038999	2311.0	8.982759642104709	38.765460347566815
2020-12-08 12:41:10	00:00:17	1.476	0.015369863	2311.0	8.982761542683182	38.765456533167075
2020-12-08 12:41:11	00:00:18	2.628	0.01620691	2312.0	8.98276725740191	38.7654527163478
2020-12-08 12:41:12	00:00:19	2.664	0.017267594	2312.0	8.982774872716368	38.76544508512224

3.3.4 Data analysis

In the data collection phase, the raw data has been collected in the interval of one-second for the total of 1795 seconds. This raw data has been treated using different statistical software's like Microsoft Excel sheet and Statistical Package for the Social Sciences (SPSS) are mainly used to for data analysis phases. The total data analysis phase contains six steps. The first one was describing the characteristics of the driving cycles data by defining the evaluation criteria. Then, the values of the seven criteria for each raw data of the driving cycle were calculated. After that, the mean values of the seven criteria for all the driving cycle data set were calculated and considered as a single driving cycle. For further analysis, principal component analysis (PCA) has been used as dimension reduction technique. The output of the principal component analysis was to identify factor scores. And using this factor score, the dimension of seven parameters have been reduced to three principal parameters. This parameter is the total time, the average velocity, and the stop number were selected for further analysis. These three parameters have been contributing a cumulative of around 78% of the total variation of the entire dataset.

Table 3. 3 Total variance extracted using principal component analysis

Component	Initial Eigenvalues			Extraction Sums of Squared Loadings		
	Total	% of Variance	Cumulative %	Total	% of Variance	Cumulative %
1	2.712	38.739	38.739	2.712	38.739	38.739
2	1.688	24.112	62.851	1.688	24.112	62.851
3	1.062	15.167	78.018	1.062	15.167	78.018
4	.898	12.835	90.853			
5	.567	8.106	98.958			
6	.070	.994	99.952			
7	.003	.048	100.000			

After factor score has been selected, the Euclidean distance between each driving cycle data was calculated using the mean values of the selected score criteria. For this purpose, a statistical method was used to find out the variation of the samples defined as Euclidean distance. Finally, we have Selected the smallest Euclidean distance for each driving cycle as it near to the mean value. This value indicates the representative of the drive cycle. the summary of data analysis phase shown Below in table 3.4.

Table 3. 4 Final selected dataset

Dataset	Distance (km)	Time (sec)	Time (h)	Max velocity(km/h)	Avarage Velocity (km/h)	Max. Acceleration (m/s2)	Max Declration(m/s2)	Stop Number	Equilidian distance
1	7.6945257	1543	0.43	61.96	17.8089	1.7	-2.06	31	1.711
2	6.092533	1910	0.53	47.3	11.3559	2.14	-1.96	42	11.633
3	9.35553	1404	0.39	58.72	23.8639	2	-2.32	30	7.844
4	7.979861	1719	0.48	67.03	16.5185	1.57	-2.81	31	0.546
5	12.53584	2108	0.59	73.48	21.1466	1.41	-2.33	37	7.508
6	7.8697715	1359	0.38	57.89	21.4048	1.72	-2.36	23	9.91
7	12.468418	1854	0.52	65.77	23.9691	1.45	-2.69	25	10.107
8	7.2197266	1236	0.34	70.09	20.6469	1.7	-2.32	17	15.088
9	4.3218837	1909	0.53	60.16	8.0356	1.43	-1.7	37	9.857
10	6.825683	1819	0.51	68.72	13.3729	1.82	-5.02	29	3.668
11	4.0448785	1900	0.53	61.06	7.679	2.02	-2.61	33	8.618
12	7.277566	2028	0.56	61.88	12.6899	1.46	-2.21	37	6.581
13	7.70736	1751	0.49	60.88	15.4636	1.4	-3.11	31	0.792
14	7.649668	2055	0.57	64.01	13.2826	1.96	-2.28	39	8.122
13	7.687361	1765	0.49	60.98	15.4656	1.7	-3.61	32	0.908
14	7.699668	2051	0.57	64.31	13.2856	2.01	-2.58	39	8.121
17	8.559839	1598	0.44	67	19.1874	1.99	-2.76	23	8.933
18	8.242806	2100	0.58	63.11	13.957	1.65	-6.43	34	8.933
19	7.875609	2423	0.67	79.06	11.2885	2.87	-3.49	36	6.693
20	8.6508255	1373	0.38	61.2	22.5182	1.95	-3.03	22	11.356
Ava.	7.888	1795.25	0.499	63.8205	16.147	1.7975	-2.88	31.4	
Std.	2.036		0.0844	6.48	4.9851	0.3461	1.107	6.64	
Var.	4.146		0.007	42.086	24.8	0.12	1.226	44.147	

3.4 Road grad identification

The road grad contributes a major impact on the energy storage system of electric vehicle. To identify and simulate the impact, these theses have been collected the topographic data of Addis Ababa Ethiopia. To do that, the thesis has been collected specific route topographic data considering the worst possible scenario. For data collection phase, direct physical survey Primary data were collected in a real-time manner using a GPS and data logger software. The data logger software is responsible for displaying the initial and final altitude coordinate points, the time taken, and the distance travelled throughout data collection time. For collection of realistic and precision of the data, 1 second sampling time has been adopted.

Table 3. 5 Primary data collected

	Distance travel	Time taken		Initial postion			Final Postion		Avargae altitude	Avargae percentile	max alt gain	Max grade %
Sidestkilo to shero meda	1540	175	2469	9.038289782	38.75484578	2543.0	9.052075724	38.75605016	74	6.60	66	8.20
Betemenegest to pm	604	79	2359	9.010571886	38.75719971	2389.0	9.015953001	38.75774878	30	4.96	25	12.00
Sheraton to pm	324.21	55	2369	9.015956732	38.75362378	2394.0	9.017165307	38.75496251	25	12.20	11	13.00
Tederos to Piyasa	498	71	2343	9.015525678	38.74569141	2383	9.020407747	38.74524939	40	3.97	25	10.80
Tederos to Piyasa_2	701.74	123	2387	9.020587922	38.74526076	2432.0	9.026432843	38.74518627	45	6.41	28	11.10
Tekuranbsa street	647	66	2352	9.019162567	38.75239956	2383	9.018738307	38.74749274	31	4.79	78	13.60
Ethio Medicen factory	667	147	2248	8.981994333	38.71961676	2266	8.986943361	38.72165327	18	5.10	45	8.30
Ruwanda street	404	45	2292	8.982243302	38.77006186	2301	8.983496381	38.77330439	9	2.36	55	13.50
Gofa to behrtsegea	360	120	2226	8.956373334	38.74567064	2248.0	8.956481361	38.74861825	22	6.11	29	12.50

Table 3.5 shows the possible uphill location candidate in the city of Addis Ababa. for the selection of candidate location, this thesis has been used prior knowledge and interview methods with different people to select candidate location in the city. After this process, the nine highest locations have been selected. Tekuranbsa (Black lion road) has been chosen as the potential highest hills location in Addis Ababa.

Figure 3. 3 Black lion road data extracted

3.2.1 Selected data

Table 3. 6 Final Selected Road Grade data

Collected data	Approximate Measured value
Distance traveled	647 m
Base point of Elevation	2352 m
Highest point of Elevation	2383 m
Elevation difference	78 m
Maximum grade	13.6

3.5 Dynamics modeling

3.5.1 Vehicle Dynamics modeling

For modeling electric vehicle dynamics and the external force associated with it, different design parameters have to be considered in the model. Since this parameter value will influence the exact behavior of the model, practical parameter values should be considered. and it is shown below in the table 3.7

Table 3. 7 variable to be assumed

N. o	Dynamics variable to be assumed	Symbol	Value taken
1	Air density at specified temperature	ρ	1.25 kg/ m3
2	Total vehicle weight, load capacity	m	1000 kg
3	Coefficient of Drag	C_d	0.3
5	Coefficient tire Rolling resistance	Crr	0.02
6	Frontal volume of the vehicle	A_f	2.0 m²
7	Max velocity of vehicle	V	67.03 km/h
8	Gravitational constant	g	9.81 m/s²
9	Diameter of the wheel	d	14 inches
10	Gear ratio	G	2
11	Regen efficiency	η	0.3
12	Assumed friction loss	μ	0.5
13	Ki,ki kw,C	Ki,ki kw,C	0.0167,0.0452,5.0e-5 and 600

3.5.2 Vehicle Longitudinal Dynamics

To move an electric vehicle forward or backward, the vehicle applied force must overcome all of the resistive forces which oppose applied force. This applied force to overcome these external forces by transferring power using the vehicle drive system is known as the total tractive force (Ftr). The model shown all these tractive & all resistive forces shown in Figure 3.4

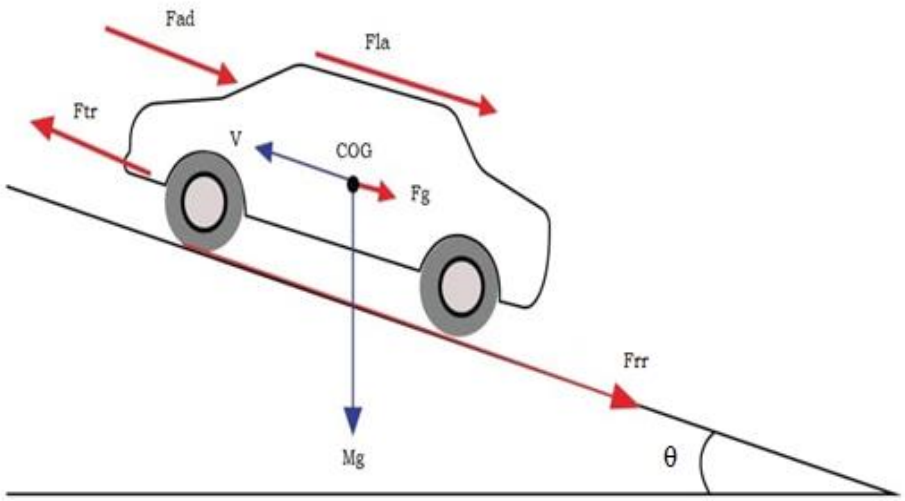

Figure 3. 4 all vehicle force representations

The total tractive force expressed as $F_{tr} = F_{la} + F_g + F_{rr} + F_{ad}$ ……..... Eq. 3.1

Where Fla is the linear acceleration force,

F_g is the gravitational force acting on the vehicle on non-horizontal roads,

F_{rr} is the rolling resistance force, and

F_{ad} is the aerodynamic drag force

3.5.2.1 Linear acceleration force, Fla

The acceleration force is the force generated by vehicle acceleration due to vehicle inertia. It is derived from Newton's second law of point mass motion and expressed as,

$$Fla = m\frac{d}{dt}V(t)dt = ma \quad \text{……..... Eq. 3.2}$$

Where a is the linear acceleration, m mass of the vehicle and V time varying tangential velocity

3.5.2.2 Gravitational force, Fg

The gravitational force depends on the slope angle of the road with respect to the distance. This force is generated due to gravity when the vehicle travels on a non-horizontal plane. When a vehicle is moving uphill, the positive force will have generated. while vehicle traveling downhill the negative force will have generated. The equation for gravitational force is expressed as,

$$F_g = \text{mg sin } \theta \ldots\ldots\ldots\ldots \text{ Eq. 3.3}$$

where θ the vehicle inclination angle is expressed in radians, m is the total vehicle mass and g is the acceleration due to gravity

3.5.2.3 Force of rolling resistance, Frr

Rolling Resistance is the energy loss inside tires due to the hysteresis effect of rubber materials and deformation of road surface [41]. When a vehicle is running on a well-prepared hard road, the effect of rolling resistance due to deformation of the road surface is significantly reduced. In this case, the only effect caused by the tire hysteresis effect will remain the same. However, in most real case scenarios, the vehicle is subjected to deformation of the road surface. Hence the impact of rolling resistance should be considered in the design part. The rolling resistance is usually taken by a rolling coefficient, Crr defined as the horizontal force acting on the wheel rotating center, which maintains the wheel rotating on a road while unit load acting on the wheel center perpendicular to the road surface as shown in Figure 3.4 it is mathematically expressed as

$$F_{rr} = \text{Mg } C_{rr} \cos\theta \ldots\ldots\ldots\ldots\ldots\ldots \text{ Eq. 3.4}$$

Where M is vehicle mass, g is gravity acceleration, Crr is the rolling resistance coefficient, and θ is the road grade angle as shown in Figure. 3.4 The coefficient of rolling resistance can be affected tire and road conditions, such as tire material, tire structure, temperature, inflation pressure, tread geometry, road roughness, and presence of liquid on the road. and rolling resistance can be taken as constant. [41].

3.5.2.4 Aerodynamic Drag Force, Fad

The aerodynamic drag force occurred on a vehicle is due to the viscous friction of the surrounding air acting on the vehicle surface and the pressure distribution behind the vehicle. This source of drug resistance depends on the shape of the vehicle, frontal area, and velocity of the vehicle. The total aerodynamic drag force is expressed as

$$F_{ad} = \frac{1}{2}\rho C_d A_f V^2 \ldots\ldots\ldots\ldots \text{ Eq. 3.5}$$

Where ρ is the air density in kg/m³ , Cd is the aerodynamic drag coefficient , Af is the vehicle equivalent frontal area in m² and V is vehicle velocity in m/s

3.6 Electric Vehicle Power and Energy Requirement

This chapter describes the power and energy requirements of electric vehicles which will be adopted in the city of Addis Ababa. The various operating modes that the vehicle is subjected to throughout a drive cycle profile are presented which will help to analyze the instantaneous tractive power requirements and net energy spending. To approximate the power and energy requirement parameters, this thesis examines the longitudinal dynamics of the vehicle. After describing the vehicle kinetics, an empirically confirmed vehicle model developed using MATLAB/Simulink is presented.

Using this vehicle model, four standard drive profiles are examined. After that, the developed Addis Ababa drive cycle are examined which will help us to study the effect of geographical location in a process of adoption of electric vehicle in case of Addis Ababa/ Ethiopia.

To illustrate the effect of arbitrating power flow for a battery and ultra-capacitor energy storage system, this thesis uses a generic built-in battery and supper capacitor model, and simulations are presented to show the vehicle power and energy demand.

3.6.1 Vehicle Propulsion Power Demand

When the vehicle is traveling, the vehicle energy storage devices supply the necessary power sources. Which is proportional to the amount of tractive force generated.

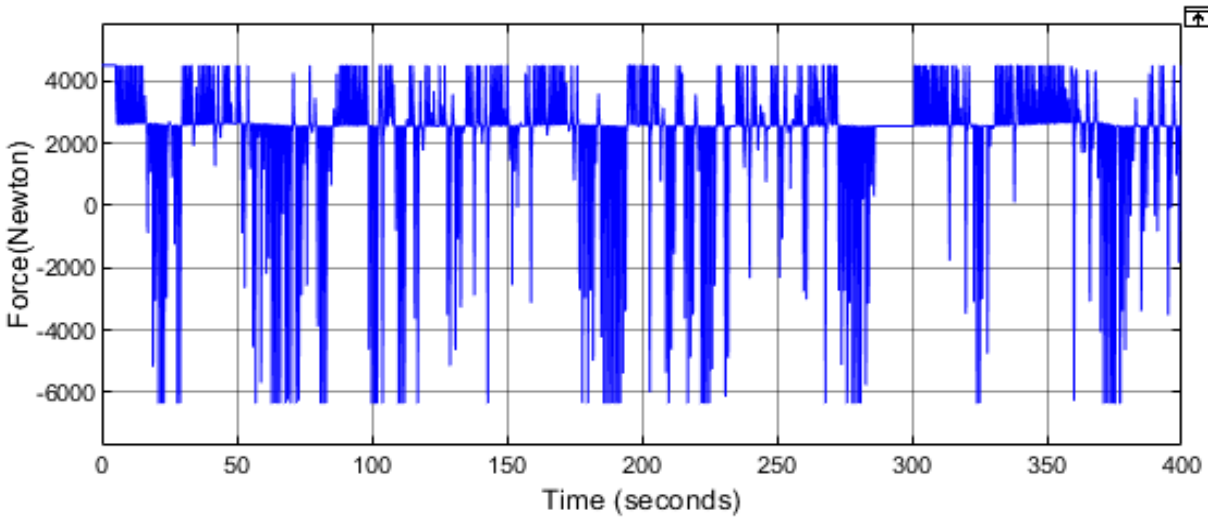

Figure 3. 5 Tractive force based on Addis Ababa drive cycle

As described above in section 3.3.2 the traction force is the sum of aerodynamic and rolling friction forces and the force due to the acceleration. And the traction force can be expressed as:

$$Ftr = ma + mgsin\theta + \frac{1}{2}\,\rho\, C_d\, AfV^2 + mgCrr \quad \text{…….. Eq. 3.6}$$

To get instantaneous tractive power using the above tractive force Ftr, it multiplied with the velocity of the vehicle, we get the instantaneous tractive power and can be expressed as

$$Ptr = ma.V + mgsin\theta.V + \frac{1}{2}\,\rho\, C_d\, AfV^3 + mgCrr.\,\text{V……. Eq. 3.7}$$

where Ptr(t) is instantaneous tractive power, Ftr(t) is total tractive force and V(t) is velocity of the vehicle.

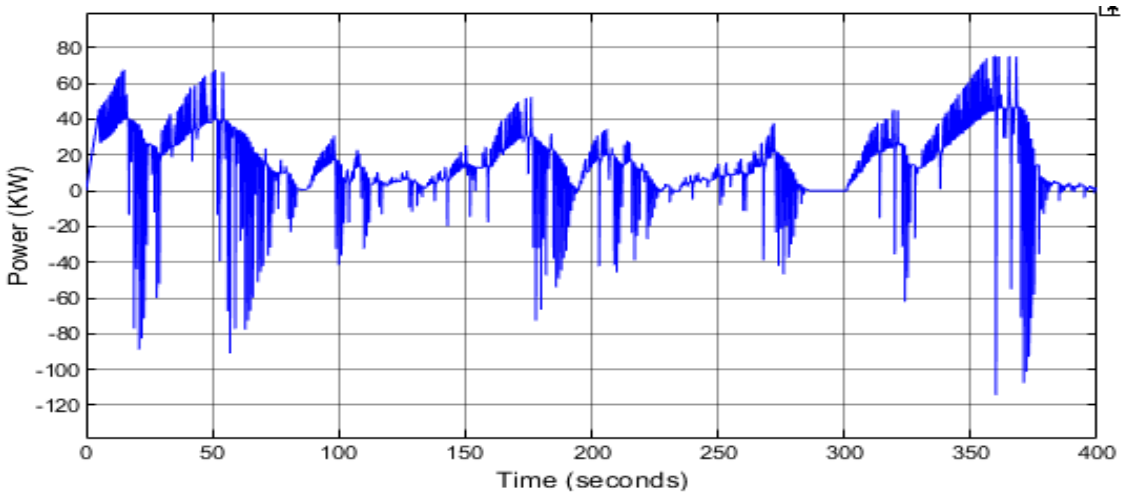

Figure 3. 6 Instantaneous Tractive Power demand Addis Ababa drive cycle

3.6.2 Vehicle Propulsion Energy Demand

Design and sizing of an energy storage system to meet the propulsion demands for a given drive profile is obtained from the energy requirement of the propulsion system. Specifically, this can be used to determine the minimal battery and ultra-capacitor size that would be able to supply and capturing available regenerative braking energy. The energy required by the propulsion load over an interval is obtained by integration of the instantaneous power equation as,

$$Etr = \int Ptr \quad \text{…….. Eq. 3.8}$$

where Etr is tractive energy and Ptr is instantaneous tractive power.

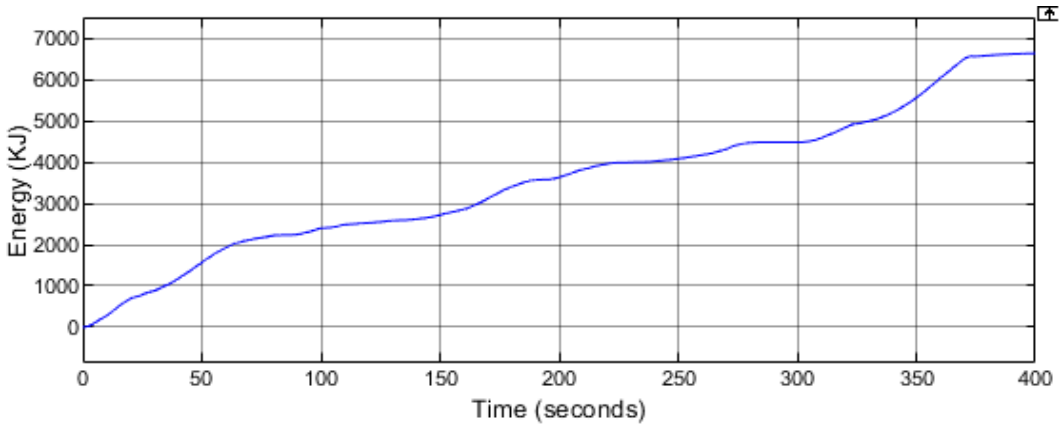

Figure 3. 7 Energy demand Addis Ababa drive cycle

3.7 Design of bi-directional buck–boost DC/DC converter

By considering tractive and regenerative energy, this thesis implements a bi-directional buck-boost DC/DC converter. It is mainly because it has the capability of acting as a boost converter when a light or heavy load is demanded. In such a case power is discharged independently from Ultra-capacitor bank and batteries bank to DC bus. Similarly, it has the capability of capturing regenerative energy when a buck converter is in operation.

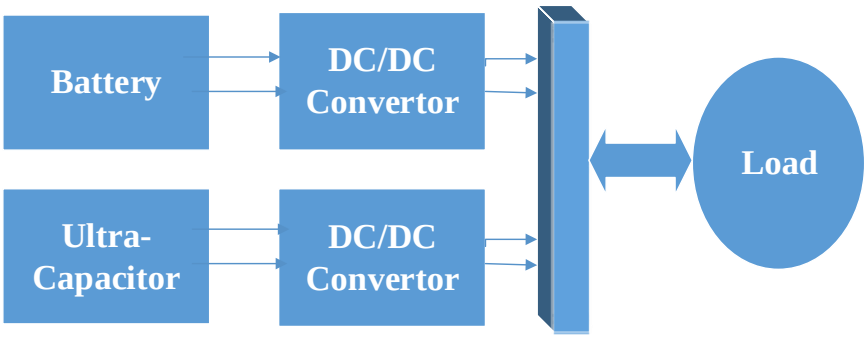

Figure 3. 8 Fully active convertor topology

Since there are different types of convertor topology, this thesis adopts fully active buck-boost convertor topology as it is suitable for interfacing batteries and ultra-capacitors as bi-directional current flow control. The theory of operation for the convertors will be explained step by step below.

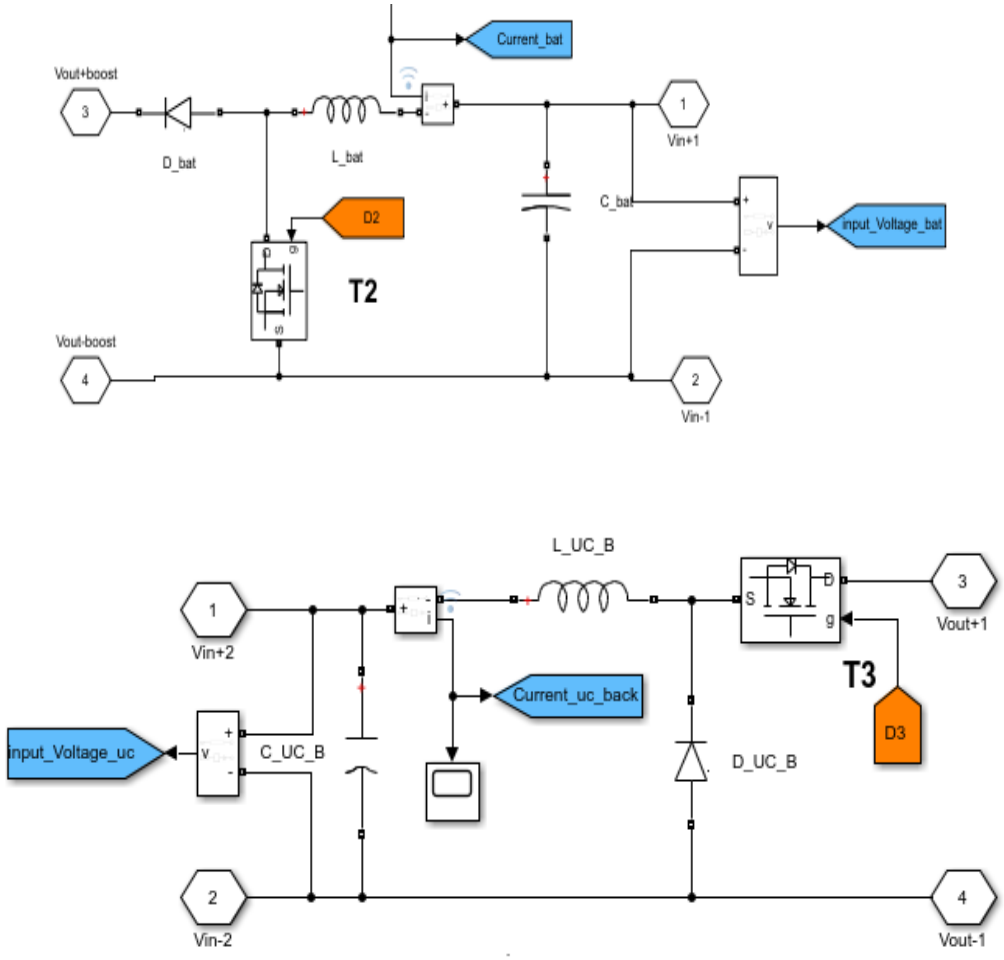

Figure 3. 9 (a) boost Convertor (b) buck Convertor topology of HESS

In case of a boost operation mode of battery, switch T2 and diode D1 will be an active circuit in vice versa and supplying positive current to the load. Since this work assumes all regenerative energy could be captured by ultra-capacitor, battery converter buck operation is not allowed. Considering converter topology for the ultra-capacitor side the transistor T4 and diode D3 responsible for boosting operation. During buck operation, transistor T3 and diode D4 are active on the ultra-capacitor side. In the case of loads that need average power demand only the battery supplies the demanded power by actively controlling boost converter transistor T2. during the regenerative event, by controlling transistor T3, the voltage in the dc bus serves as input to the buck convertor ultra-capacitor. as a result, this will charge energy storage system specifically ultra-capacitors bank. In the case of heavy load conditions, both ultra-capacitor and batteries must responsible for supplying demanded power. this can be realized by operating both sides of the converter in boost mode by actively controlling transistor T2 and T4. For converter

operation, we use a switching frequency of 1khz. The transistors T1 to T4 are controlled by variation of duty cycle switching frequency (FSW).

3.8 Control approach for coordination between battery /ultra-capacitor ESS

The power split between battery and ultra-capacitor in the application of electric vehicles is described below.

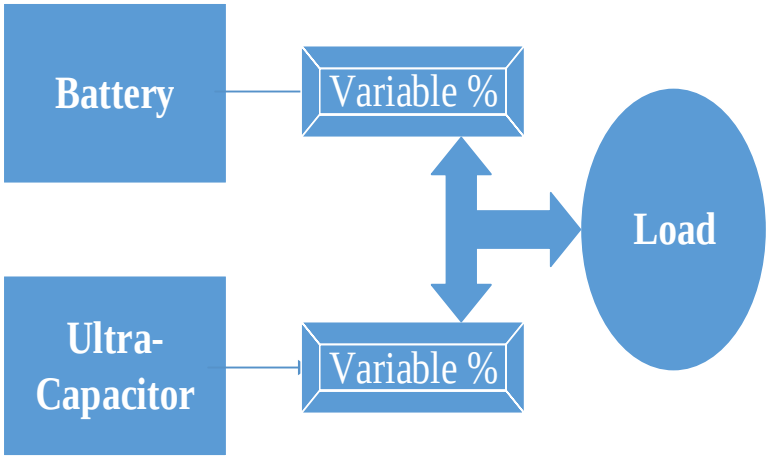

Figure 3. 10 Power and energy split between two sources

Since the load behavior highly varies with different factors, the supply power should have dynamically been varying as well. To cope up with this dynamics behavior and fulfill the load demand as needed, as well as for the successful operation of the vehicle, the power availability of the energy storage device must at least meet the power requirement. this has to be done with further consideration of energy storage devices Specifically, the state of charge (SOC) of batteries and ultra-capacitors must be frequently measured and feed to the controller which is responsible for to power split between energy storage systems. For the controllable converter operation explained above, we implement a fuzzy knowledge-based controller. Knowledge-based fuzzy controller is responsible for successful Power coordination between batteries and ultra-capacitor bank based on the load demand.

3.8.1 Modes of operation and control strategy

As it is shown in the figure above, Addis Ababa drive cycle has different modes of operation, which can be categorized in acceleration mode, Constant speed and braking mode.

3.8.1.1 Traction mode

As a design approach battery is the primary energy source so that most of the power requests are met by the battery depending on its SOC status. And the remaining power requirements are met by the ultra-capacitors through the bi-directional DC/DC converter. Based on the SOC of batteries/ultra-capacitor and requested power demand, the fuzzy controller supplies power to the system which needs to be variable reference power for the converter. And this coordination of battery and ultra-capacitor in different modes of operation is governed by the implementation of the fuzzy logic-based power management system as rules.

3.8.1.2 Braking mode

The regenerated power in the DC buss during braking has been controlled to flow back to any of the Ultra-capacitor pack only and it's because the ultra-capacitors have high power density compared to batteries and capable of capturing all available regenerative energy quickly.

3.8.2 fuzzy logic control strategy

In this study, we will adopt control strategies to coordinate power distribution between energy storage of electric vehicles which is comprised of batteries and ultra-capacitors. This control strategy will improve efficiency of energy storage and this will extend the battery's life.

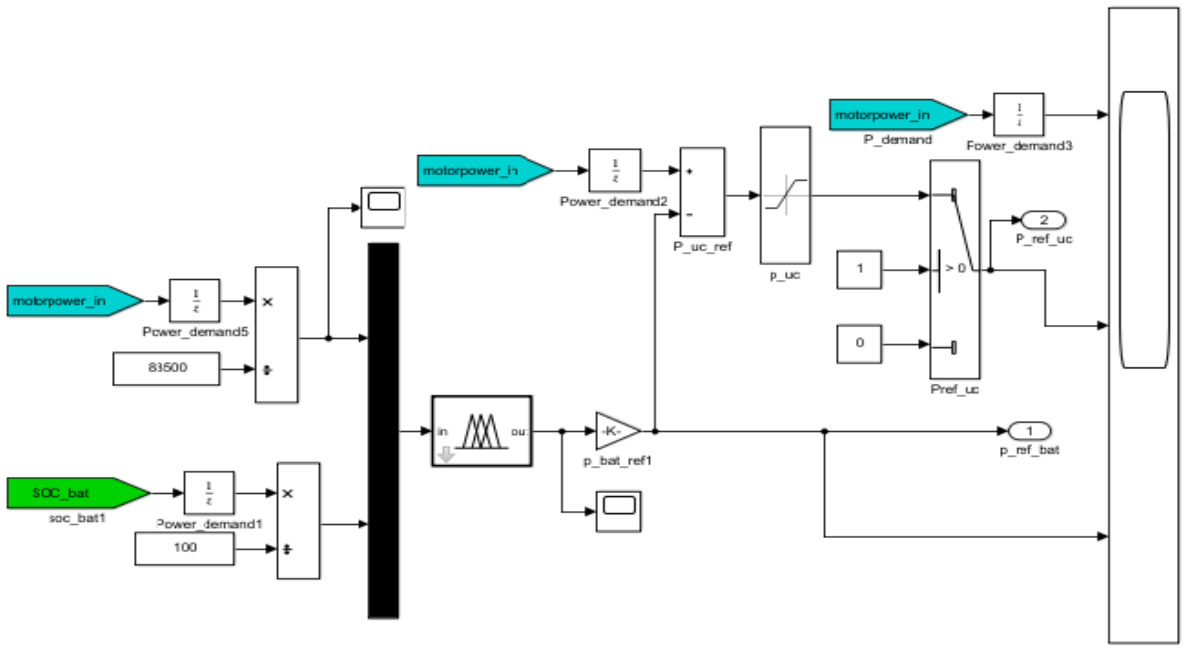

Figure 3. 11 fuzzy logic control structure

To adopt the Mamandi type fuzzy control algorithm, we will pass through several steps. First, it needs to define the membership of each key status: power demand, SOC of batteries, and SOC of Ultra-capacitors as inputs and the power distribution between the Ultra-capacitors and the battery, as outputs. Then it defines the rules based on experience and finally, it finishes the de-fuzzification based on the output membership function. Below in figure 3.12 classification of input and output membership function is shown.

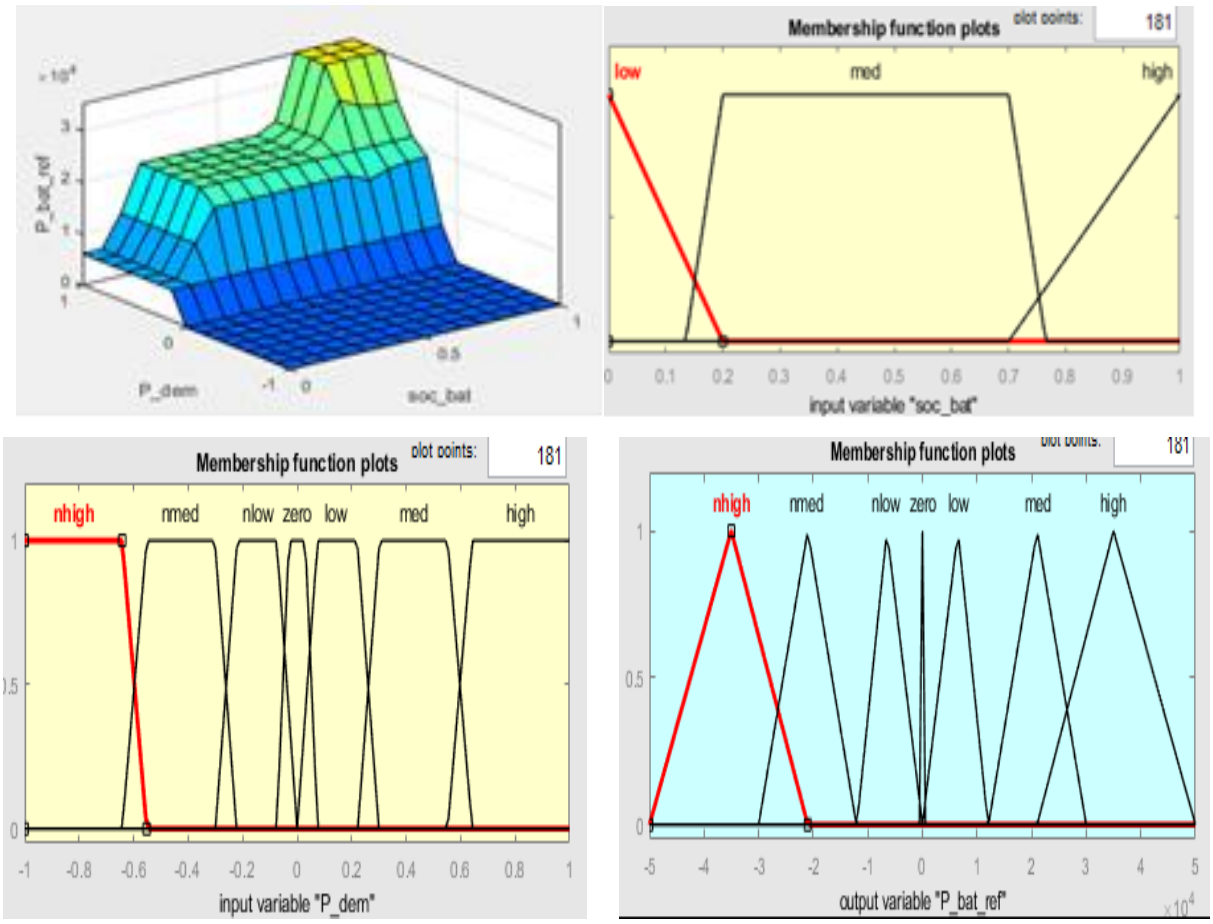

Figure 3. 12 (a) Surface (b) battery SOC membership (c) demand membership (d) output membership function of FLC.

Chapter Four: Result and Discussion

4.1 Overview

Simulations were performed to verify the feasibility of the proposed control system with the designed and modeled system components, explained in the above section. The overall design layout and block diagram of control of the proposed control system for electric vehicle application are shown in Figures 3.1. Throughout the process, the proposed system has been adopted the constructed drive cycle of Addis Ababa/ Ethiopia as a reference speed profile and the PI controller has been used to track the velocity of the vehicle in the given drive cycle.

First, the battery-alone system has been considered and used in the model as an energy source. And the power demanded by the electric vehicle throughout the time has been supplied by the battery source alone, and this will force the battery system to provide all power during tractive and receives all power during regenerative braking events. Initially, the SOC of the battery was 100% with its equivalent maximum DC-link voltage. The battery current, its SOC, and the distribution of motor and battery power are shown below in Figure 4.4. For this duty, the pick current drawn from the battery was 237.5 Ampere. And the SOC drops from an initial 100% to 79.89 % for a given Addis Ababa drive scenario.

By hybridizing both battery and UC as energy sources; the main source battery is limited to provide maximum power of 58 KW and the auxiliary source UC has been controlled to provide the remaining 25 kW power. And additionally, only UC has been allowed to capture all available regenerated energy during deceleration, which mainly depends on the SOC condition of UC. Figure 4.5 shows the obtained responses of battery and UC for a hybridized system with the proposed control strategy. And it is shown that the pick battery current of the hybridized system is nearly 167.1 Ampere. It was found that less magnitude of current has been drawn from the battery pack. The UC-rated voltage was 330V at its 100% SOC. For efficient operation and reduction of electrical Struss of ultra-capacitors, voltage variation has been maintained in between its minimum value of 30% and its maximum value of 95%. Therefore, at 30% SOC, UC voltage becomes 100 V and at 95% SOC UC voltage value is 317 V for its efficient operation. For the given Addis Ababa drive cycle test scenario, the initial SOC of UC is around 80%. Because of the frequency of acceleration and deceleration in the drive cycle, the SOC falls and rises frequently and the aggregate value of UC SOC reaches 90% at the end of 400 s.

4.2 Comparison between different drive cycle

Table 4. 1 comparison between different drive cycle 100% regeneration efficiency

No	Test Cycle	Description	Tractive	Regenerative	Net
1	Addis Ababa	Pick Power	75 KW	-167 KW	
		Propelling Energy	6943 KJ		
		Braking Energy		-307.8 KJ	
		Net Energy	6635KJ		
		SOC (Batt only)	100 – 79.8% (20.18 %)	100 – 81.45% (18.55%)	1.63%
2.	HUDDS	Pick Power	66.99 Kw	-137 Kw	
		Propelling Energy	2977 KJ		
		Braking Energy		-183.5KJ	
		Net Energy	2793 KJ		
		SOC (Batt only)	100- 85.45% (14.55%)	100- 86.31% (13.69%)	0.86%
3	NY Composite	Pick Power	30.93 Kw	-57.5 Kw	
		Propelling Energy	664.9KJ		
		Braking Energy		-84.80 KJ	
		Net Energy	580.1KJ		
		SOC (Batt only)	100- 89.19% (10.81%)	100- 89.32% (10.68%)	0.13%
4	NYCC	Pick Power	51.60 KW	-111.7 KW	
		Propelling Energy	3047KJ		
		Braking Energy		-235KJ	
		Net Energy	2813KJ		
		SOC (Batt only)	100 – 85.51% (14.49%)	100 – 86.52% (13.48%)	1.01%
5	WLTP class 1	Pick Power	47.73 KW	-93.3 KW	
		Propelling Energy	5387KJ		
		Braking Energy		-50.87 KJ	
		Net Energy	5336KJ		
		SOC (Batt only)	100-80.80 % (19.2%)	100 – 81.09% (18.91%)	0.29%
6	WLTP class 2	Pick Power	61.20 KW	-120 KW	
		Propelling Energy	5147KJ		
		Braking Energy		-115.7KJ	
		Net Energy	5031 KJ		
		SOC (Batt only)	100 – 81.83% (18.17%)	100 – 82.79% (17.21%)	0.96%
7	NEDC	Pick Power	61.4 KW	-114 KW	
		Propelling Energy	4442KJ		
		Braking Energy		-165.4KJ	
		Net Energy	4276		
		SOC (Batt only)	100 - 82.95% (17.05%)	100 – 84.03% (15.97%)	1.08%
		Fgrade	1962N		

Table 4. 2 Comparison between different drive cycle at 30% regeneration efficiency

No	Test Cycle	Description	Tractive	Regenerative	Net regen
1	Addis Ababa	Pick Power	75 KW	-114 KW	
		Propelling Energy	6919 KJ		
		Braking Energy		-281.3 KJ	
		Net Energy	6637KJ		
		SOC (Batt only)	100 – 80% (20 %)	100 – 80.6% (19.4%)	0.6%
		Fgrade	2350N		
2.	HUDDS	Pick Power	66 Kw	-98 Kw	
		Propelling Energy	2977 KJ		
		Braking Energy		-174.6KJ	
		Net Energy	2800 KJ		
		SOC (Batt only)	100- 85.5% (14.5%)	100- 85.8% (14.2%)	0.3%
		Fgrade	1962N		
3	NY Composite	Pick Power	3100Kw	-41.5 Kw	
		Propelling Energy	660KJ		
		Braking Energy		-83.2 KJ	
		Net Energy	570KJ		
		SOC (Batt only)	100- 89.4% (10.6%)	100- 89.6% (10.4%)	0.2 %
		Fgrade	1962N		
4	NYCC	Pick Power	50 KW	-80 KW	
		Propelling Energy	3000KJ		
		Braking Energy		-220KJ	
		Net Energy	2800KJ		
		SOC (Batt only)	100 – 85.6% (14.4%)	100 – 86 % (14%)	0.4%
		Fgrade	1962N		
5	WLTP class 1	Pick Power	47.5 KW	- 67 KW	
		Propelling Energy	5387KJ		
		Braking Energy		- 49.4 KJ	
		Net Energy	5336KJ		
		SOC (Batt only)	100-81 % (19%)	100 – 80.97 (19.03%)	0.03%
		Fgrade	1962N		
6	WLTP class 2	Pick Power	60 KW	-86 KW	
		Propelling Energy	5190KJ		
		Braking Energy		-111.5KJ	
		Net Energy	5000 KJ		
		SOC (Batt only)	100 - 82% (18 %)	100 – 82.3% (17.7%)	0.3%
		Fgrade	1962N		
7	NEDC	Pick Power	50 KW	-80 KW	
		Propelling Energy	4435KJ		
		Braking Energy		-158.6 KJ	
		Net Energy	4275		
		SOC (Batt only)	100 - 83% (17%)	100 – 83.4% (16.6%)	0.4%
		Fgrade	1962N		

Table 4. 3 Comparison between different drive cycle at 50% regeneration efficiency

No	Test Cycle	Description	Tractive	Regenerative	Net regen
1	Addis Ababa	Pick Power	75 KW	-129.5 KW	
		Propelling Energy	6929 KJ		
		Braking Energy		-292.6 KJ	
		Net Energy	6636.5KJ		
		SOC (Batt only)	100 – 80% (20 %)	100 – 80.91% (19.09%)	0.91%
		Fgrade	2350N		
2.	HUDDS	Pick Power	66 Kw	-104.5 Kw	
		Propelling Energy	2977 KJ		
		Braking Energy		-177.5KJ	
		Net Energy	2793.5 KJ		
		SOC (Batt only)	100- 85.5% (14.5%)	100- 86.02% (13.98%)	0.52%
		Fgrade	1962N		
3	NY Composite	Pick Power	31Kw	-44.7 Kw	
		Propelling Energy	664KJ		
		Braking Energy		-83.65 KJ	
		Net Energy	580KJ		
		SOC (Batt only)	100- 89.4% (10.6%)	100- 89.41% (10.59%)	0.01%
		Fgrade	1962N		
4	NYCC	Pick Power	50 KW	-85 KW	
		Propelling Energy	3037KJ		
		Braking Energy		-226KJ	
		Net Energy	2812KJ		
		SOC (Batt only)	100 – 85.6% (14.4%)	100 – 86.25% (13.75%)	0.29%
		Fgrade	1962N		
5	WLTP class 1	Pick Power	47.5 KW	- 71.2 KW	
		Propelling Energy	5386KJ		
		Braking Energy		- 50 KJ	
		Net Energy	5336KJ		
		SOC (Batt only)	100-81 % (19%)	100 – 81.02% (18.98%)	0.02%
		Fgrade	1962N		
6	WLTP class 2	Pick Power	60 KW	-91.65 KW	
		Propelling Energy	5144KJ		
		Braking Energy		-112.9KJ	
		Net Energy	5031 KJ		
		SOC (Batt only)	100 - 82% (18 %)	100 – 82.54% (17.46%)	0.54%
		Fgrade	1962N		
7	NEDC	Pick Power	61.4 KW	-88.2 KW	
		Propelling Energy	4437KJ		
		Braking Energy		-160 KJ	
		Net Energy	4277		
		SOC (Batt only)	100 - 83% (17%)	100 – 83.55% (16.35%)	0.65%
		Fgrade	1962N		

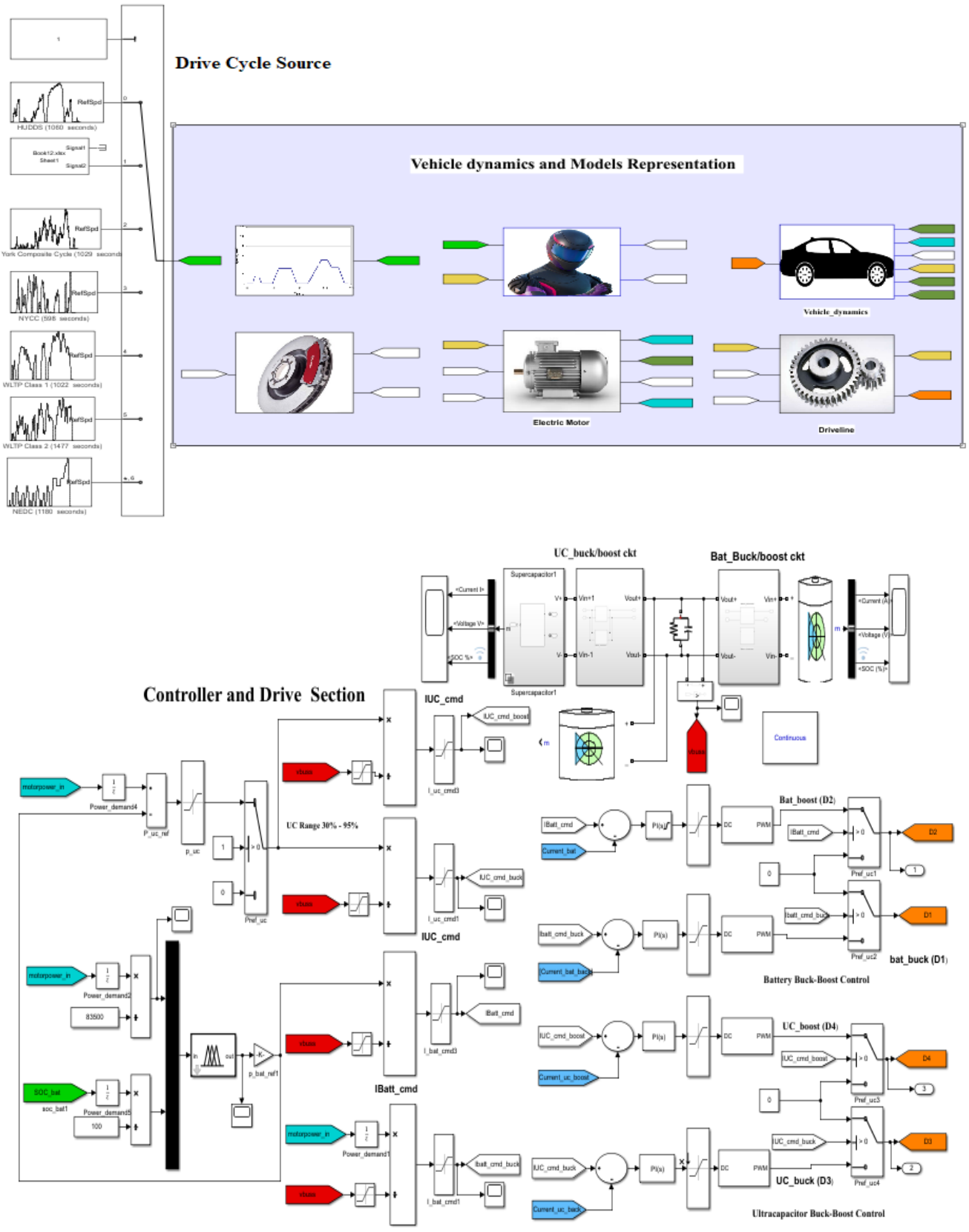

Figure 4. 1 (a) block diagram (b) control and drive overall system overview

Based on the SOC of the energy storage system and power demand of vehicles, the fuzzy logic controller generates reference power to the PI controller. Both figure 4.2 and 4.3 shown below is highly varying reference power generated from the fuzzy logic controller. It is seen in the figure that, the first one is the plot for power demand needed which is generated from the dynamic model of the vehicle. Considering 30% of regeneration efficiency for the case of the Addis Ababa drive cycle, the pick tractive power demand needed is around 83KW power and 21KW power for regeneration in figure 4.2. On the other side, in figure 4.3 shown below, the ultra-capacitor bank will not contribute any power to the load. Hence the reference power from fuzzy logic control is zero.

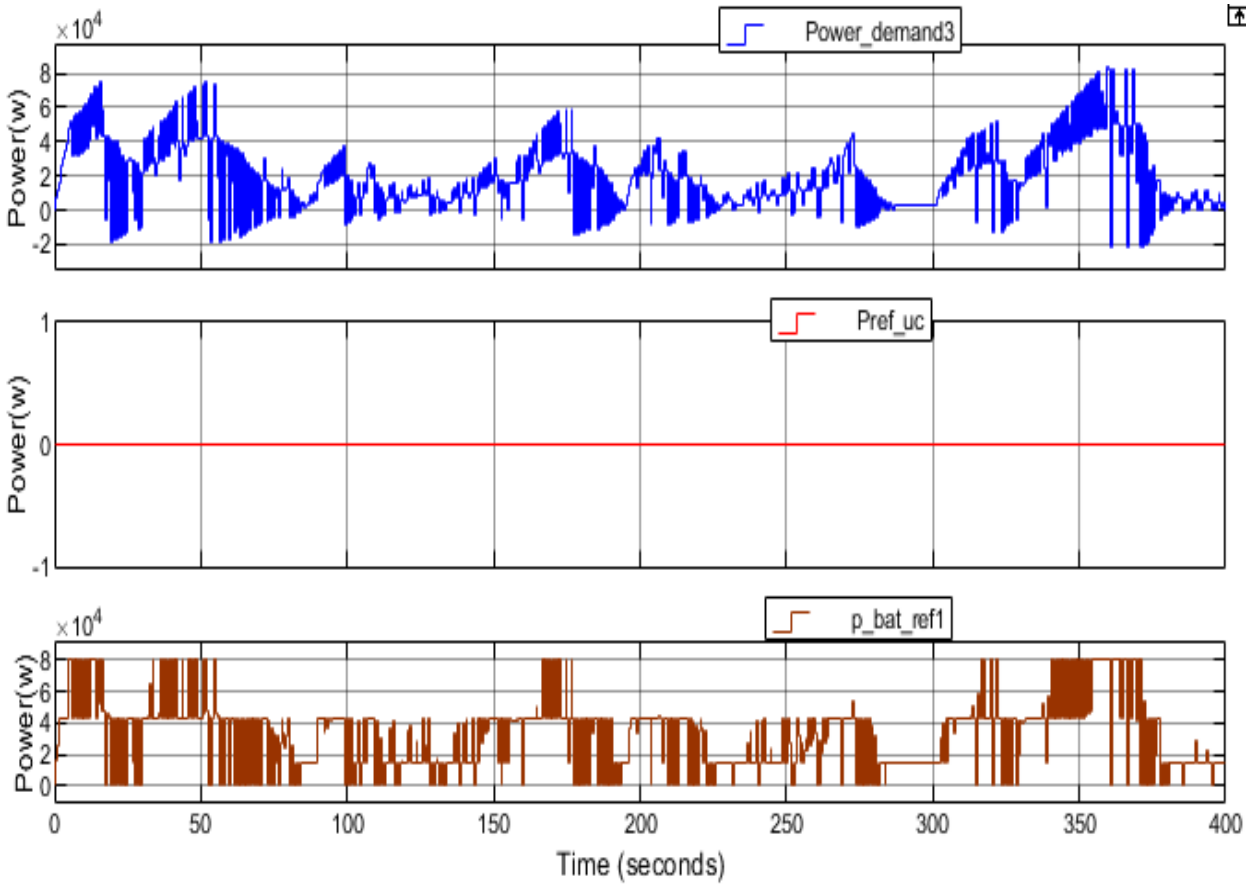

Figure 4. 2 (a) power demand (b) UC power (C) battery reference of FLC of BESS system

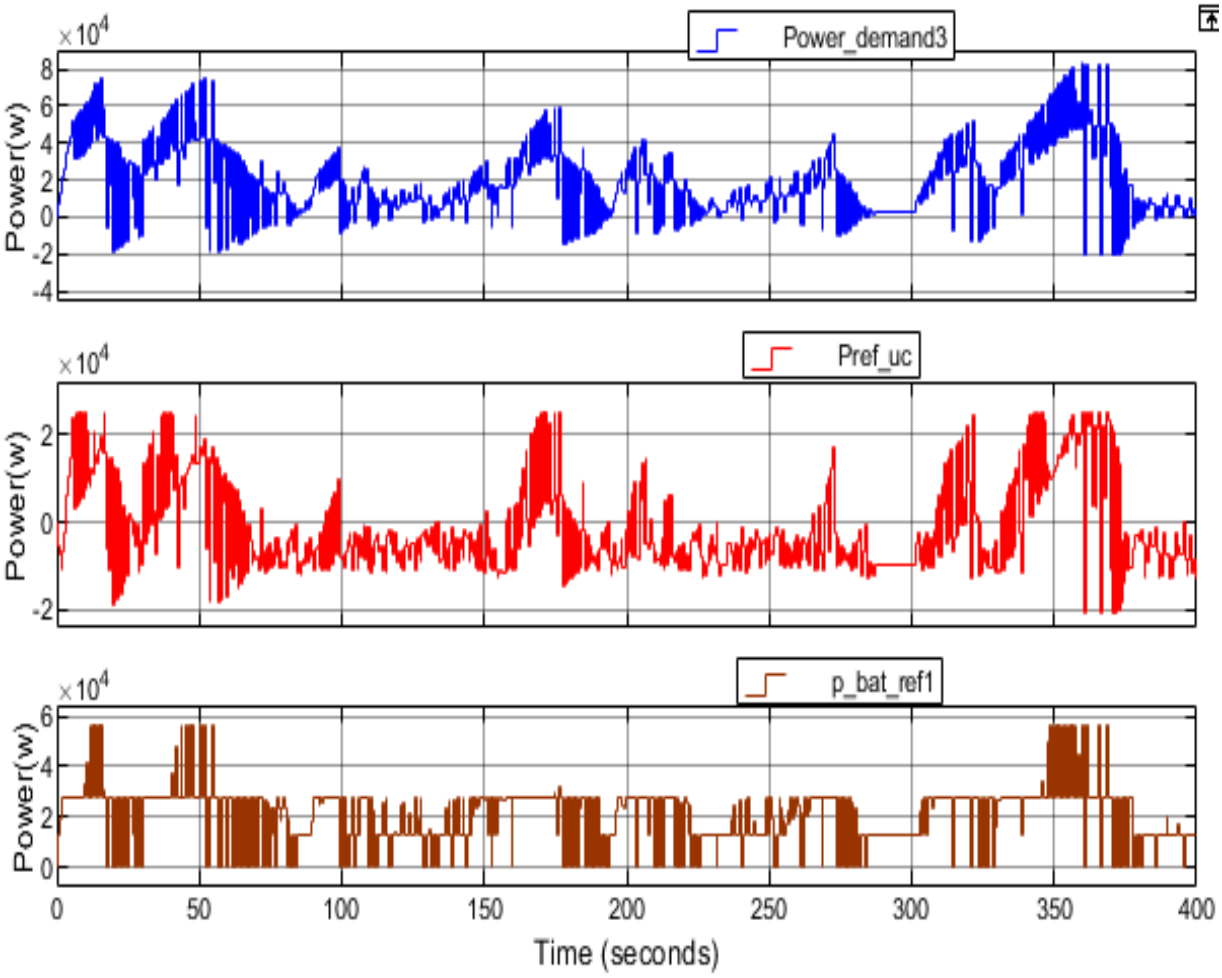

Figure 4. 3 (a) power demand (b) UC power (C) battery reference of FLC of hybrid system

The second plot is reference power to be supplied from the Ultra-capacitor bank. For this thesis, it is assumed that the ultra-capacitor will contribute a maximum of 25KW pick power to the load in case of tractive power needed and 21KW of pick power will be consumed in case of regeneration. Lastly, for the battery pack reference power, around 58KW of pick power will be delivered to the load during traction mode of the vehicle and because of the nature of ultra-capacitor high power density characteristics, our approach to storing all regenerative energy in the ultra-capacitor. Hence, the battery will not store regenerative energy. All regenerative energy will be stored in an ultra-capacitor pack.

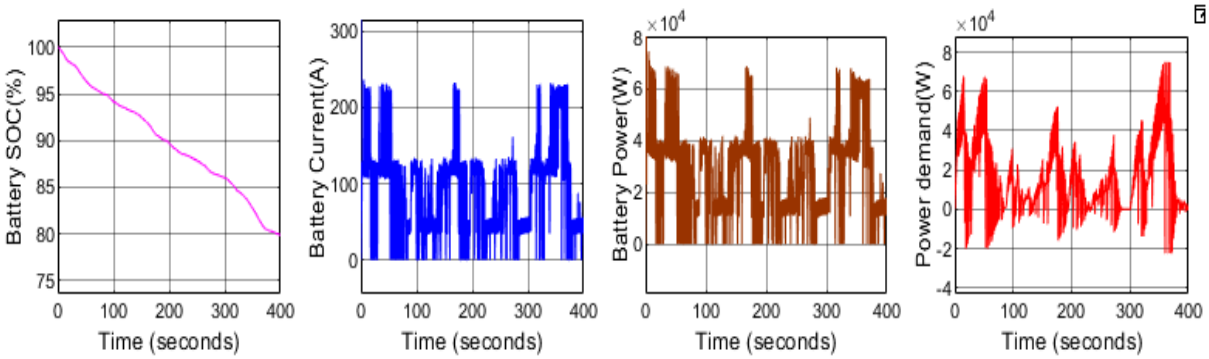

Figure 4. 4(a) battery SOC,(b)battery current,(c)battery power voltage and (d)demand BESS

To check the geographical and road grad impact on energy storage systems, in the case of the adoption of electric vehicles in Addis Ababa, we have modeled electric vehicle and batteries and ultra-capacitor packs using mat lab/Simulink environment, and the feasibility study is conducted based on the simulation performance test. The first simulation of the model is performed in the assumption that the demanded power during tractive mode is supplied by battery alone that is the energy storage system only contains battery pack alone. In this case, the batteries should be capable of delivering the pick power demand that comes from the road dynamics. figure 4.4 shows the current, voltage, and SOC distribution of the battery alone energy storage system. And it is shown that initially the battery fully charged that is SOC 100% and after running 400-second simulation the battery SOC is discharged to 80%. During simulation time, the pick battery current reaches is nearly 230A and it is clearly shown that battery power can be capable of meeting all the demanded power.

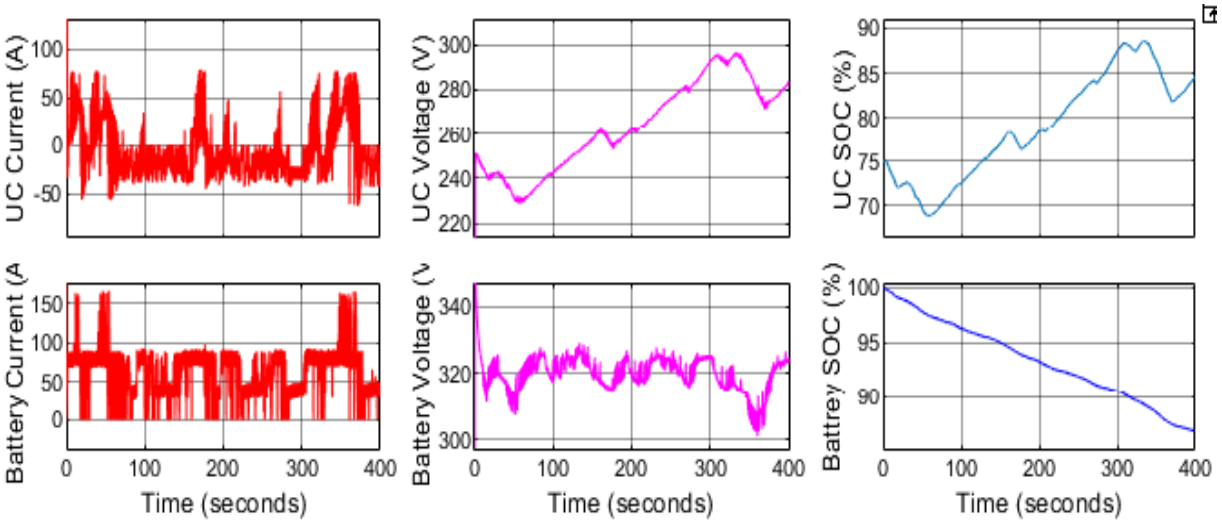

Figure 4. 5 a) UC current b) UC voltage c) UC SOC d) battery Current e)battery Voltage

f) battery SOC HESS

For a hybrid Energy storage system, it is assumed that the demanded power during tractive mode is supplied by both battery pack and ultra-capacitor pack. It is to means that the energy storage system contains a battery pack and ultra-capacitor pack. In this case, both energy storage devices should be capable of delivering the pick demand power that fulfills the given drive cycle dynamics. Figure 4.5 shows the current, voltage, and SOC distribution of both battery and ultra-capacitor packs. And it is shown that initially the battery is fully charged that is SOC 100% and ultra-capacitor initial SOC is 75%. After running 400-second simulation the battery SOC is discharged to 86.8%. Due to city geographical landscape & road contour convenience for regenerative energy. The ultra-capacitor SOC capturing additional 10% SOC that is 85% SOC. during this time, the pick batteries current reaches are nearly 160A, and the capacitor current supply the remaining current demand in case of tractive mode. The pick magnitude of the ultra-capacitor current reaches nearly 77 amperes. Based on available regenerative energy, it will capture all current related to regenerative energy and its peak magnitude reaches 62 amperes.

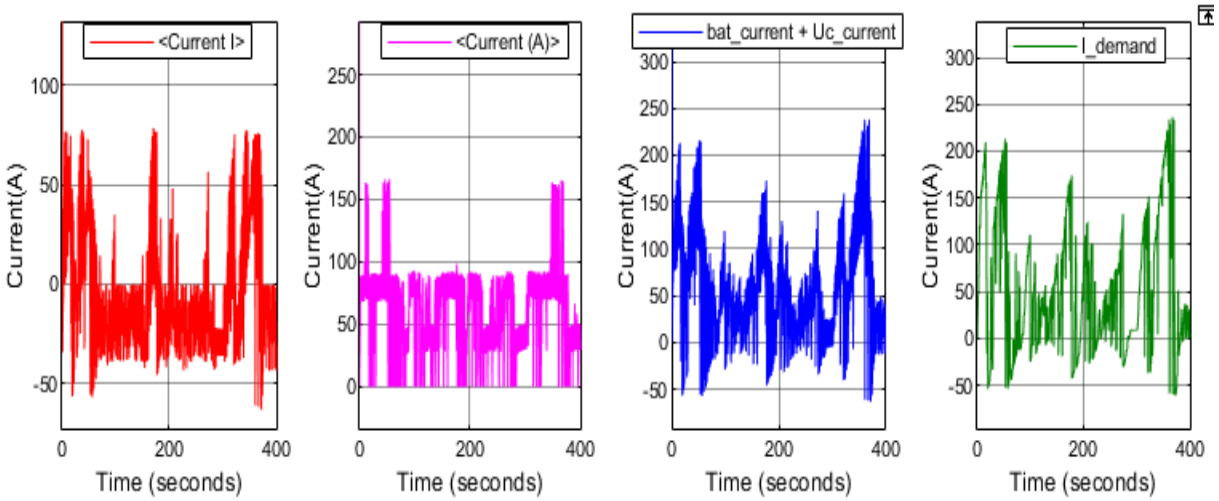

Figure 4. 6 a) battery current, b) ultra-capacitor current c) hybrid current d) demanded current

In figure 4.6 above ultra-capacitor current, battery current, hybrid energy storage current, and the demanded current are shown. The magnitude of pick energy storage current (battery and ultra-capacitor) is nearly 240 amperes. It is clearly shown that the energy storage current is capable of supplying demanded current from the given drive cycle.

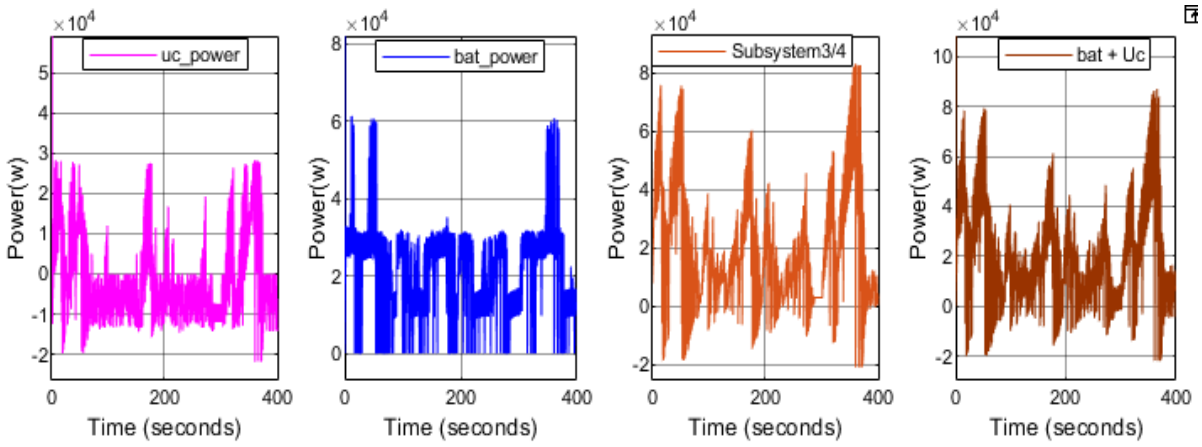

Figure 4. 7 (a) UC Power, (b) battery Power, (C) power demand and (d) hybrid system

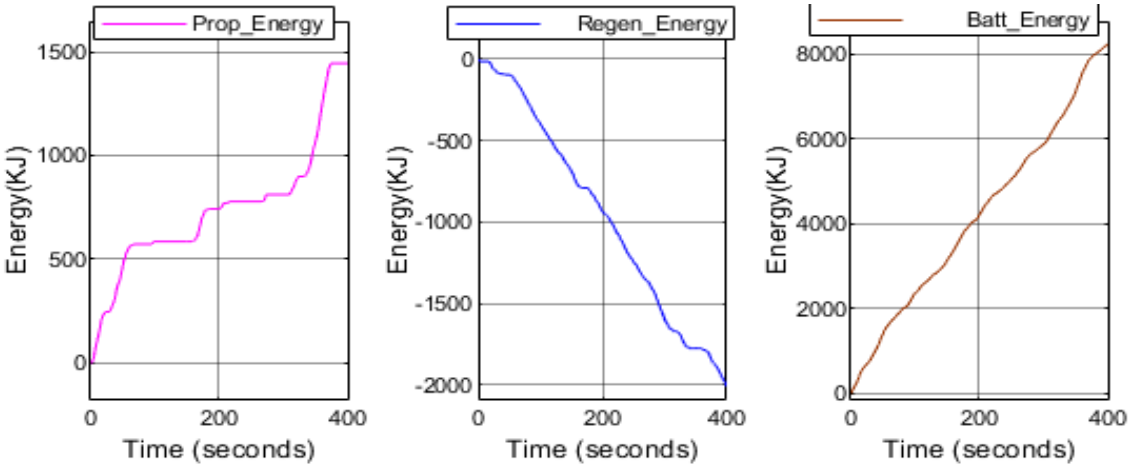

Figure 4. 8 (a) Propelling Energy, (b) regenerative Energy and (c) battery energy

In figure 4.7, it is justified that, the total power demand of the vehicle is satisfied. The energy provided by the battery and UC for the given Addis Ababa drive cycle is shown in Figure 4.8 above.

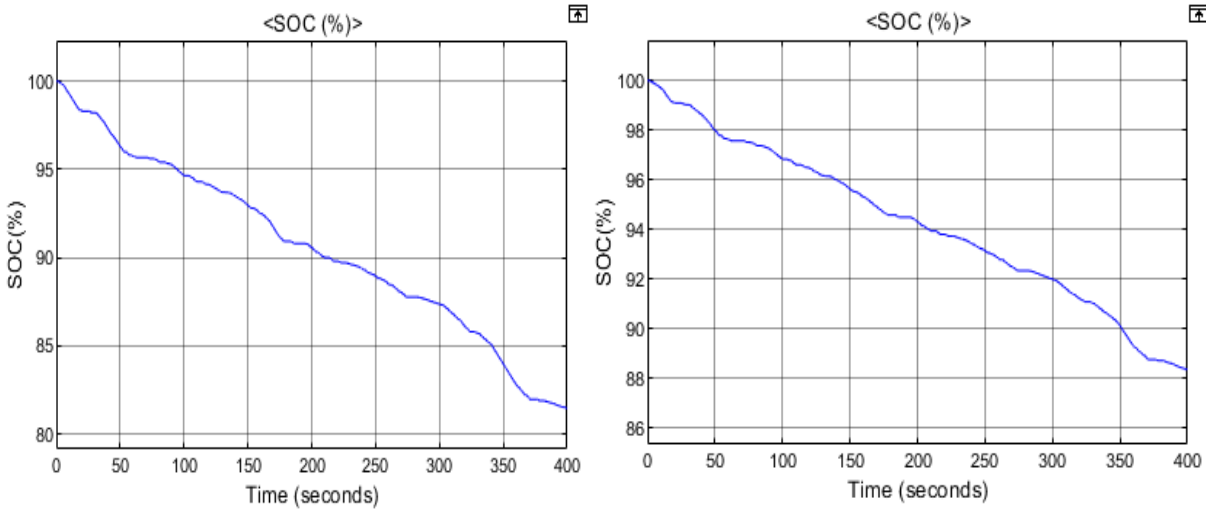

Figure 4. 9 SOC distribution (a) battery alone and (b) hybrid system SOC distribution

It is clearly shown that, the difference between battery alone system and hybrid energy storage system in terms of SOC of battery's pack shown above in figure 4.9. And we have found around 10% SOC deviation between the two systems for the given 400-second duration drive cycle is found.

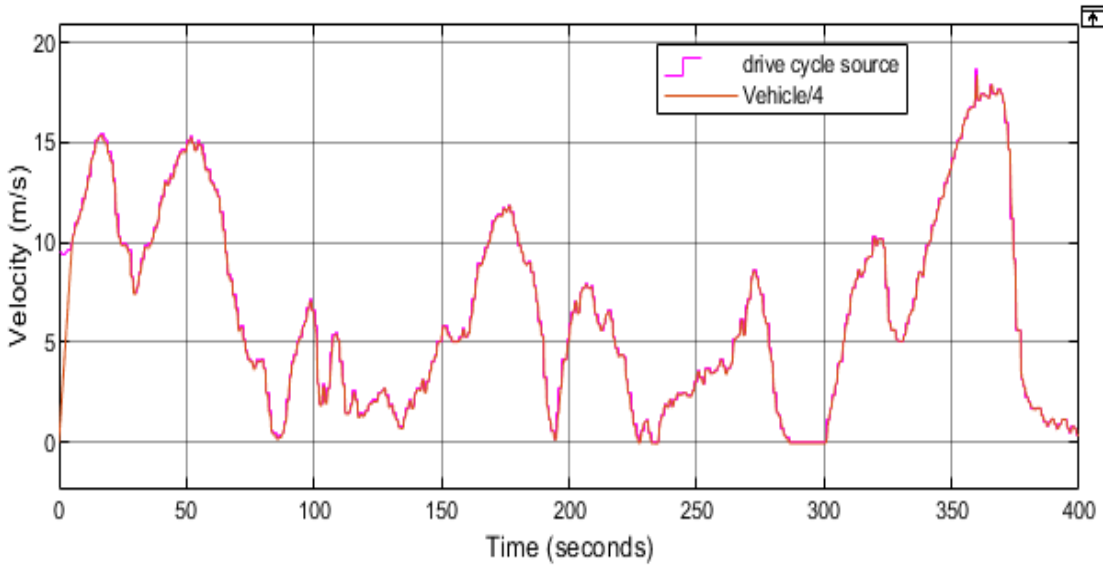

Figure 4. 10 drive cycle vs vehicle speed plot

To maintain the proper operation of electric vehicles for the given drive cycle, the speed of the vehicle in all modes of operation (tractive, idling & regenerative) should be controlled. To do that, a PI controller is adopted to simulate driver behavior. The PI controller (driver model) helps in accurate tracking of the desired speed profile. Thus, the desired and actual speed profiles of the vehicle will be the same and shown in Figure 4.10

4.3 Comparison between battery alone and hybrid systems

Generally, the performance of the proposed system is compared with the battery-alone energy storage system in terms of different performance parameters presented in Table 4.4 below. It is clearly shown that the SOC of battery, pick battery energy, pick battery current and the root mean square (RMS) current, is found to be less in the proposed system which has a significant effect on the reliability of the battery pack found in the energy storage system. So that it increases range of the vehicle and reduces the degradation of the battery caused by frequent charge-discharge cycle and hence improves its lifetime.

In conclusion, the proposed hybrid energy storage system (HESS) with the proposed control strategy reduces the pick battery current and RMS current of the battery and offers efficient power train operation. therefore, the SOC of the battery and energy delivered by the battery is reduced. This will improve the lifetime of the battery and the range of the vehicle will be increased. thus reducing the replacement cost, maintenance, and operational cost.

Table 4. 4 Comparison between battery alone and hybrid system

No	Description	Battery alone system	Battery and UC Hybrid system
1.	Peak battery current (A)	237.5	167.1
2	Battery RMS current (A)	136.7	76.73
3	Peak battery Energy	13,000KJ	8,245KJ
4	Battery SOC	Initial = 100and Final = 79.89 % deviation = 20.11%	Initial = 100 and Final = 86.86% deviation = 13.14%
5	Peak Ultra-capacitor Current (A)	-	78.62
6	Ultra-capacitor SOC	-	Initial = 80% and Final = 90 % deviation = 10 % gain
7	Peak Ultra-capacitor Energy	-	- 565 KJ
8	Ultra-capacitor RMS Current (A)	-	51.14

4.4 Comparison between different drive cycles

In this thesis, a Different comparison has been made to analyze the impact of traffic road dynamics in the cases of Addis Ababa/ Ethiopia. And based on this data simulation has been carried out. And from the result, it was found that the acceleration and deceleration magnitude is very large compared to other drive cycles. In addition to that, the magnitude of the stop number thorough runtime of the vehicle is large. This leads to an increase in the frequency of acceleration and deceleration rate. Thus, the energy storage system has been affected. Below in Table 4.5 shows the parameter data of different drive cycle

Table 4. 5 Comparison between different drive cycle

Criteria	UDDS	NEDC	EUDC	WLTP	NYCC	NY	ADDIS
Time (sec)	1369	1184	400	1800	598	1029	1719
Distance (KM)	12.0	10.93	6.95	23.27	1.89	4.02	7.97
Max Velocity (m/s)	91.2	120	120	131.3	12.3	16.1	67.03
Ava Velocity (m/s)	31.5	33.21	62.44	46.5	4.0	3.91	16.51
Max acceleration(m/s^2)	1.5	1.06	0.83	1.66	0.46	0.21	1.57
Max deceleration(m/s^2)	-1.5	-1.39	-139	-1.5	-0.48	-0.25	-2.81
Stop number	17	13	1	13	7	14	31

Chapter Five: Conclusion and Recommendation

5.1 Conclusion

In the thesis, the impact of topographic distribution and road dynamics for the adoption of electric vehicles in the case of Addis Ababa/Ethiopia has been studied. The electric vehicle model was developed and different scenarios have been tested. After the model was developed; different international drive cycles have been tested like EUDC, NYCD, and WLTP. From the simulation, it was found that; the acceleration-deceleration rate of Addis Ababa city was larger than the others. Hence, the energy consumption of electric vehicles is significantly affected. Because of this nature of the city; Electric vehicle implemented in the city suffers from the limited driving range and reduced lifetime of batteries.

On the other side, due to the topographic layout; the frequency of ups and downs of the city is larger. The possibility of regenerative braking events is significant for the efficiency improvement of energy storage. For justification concerning regenerative braking energy efficiency, the model was simulated step by step using various international standard drive cycles. And it was concluded that characteristics of the Addis Ababa drive cycle have been suitable for capturing regenerative braking energy. To overcome these challenges and improve the range of vehicles, this thesis implemented hybrid energy storage (HESS). The system incorporated lead-acid batteries in conjunction with ultra-capacitor packs. It was found from the proposed model is that; the peak RMS current has been significantly reduced. And the state of charge of the batteries has been improved. And it was described that the possible extension of the lifespan of battery and range of vehicle can be achieved.

By testing the effect of geographical landscape and road dynamics in the process of adoption of electric vehicles in Addis Ababa, this study founded that, the city road dynamics and topographic distribution indeed have a significant effect on the efficiency and range of the energy storage system of an electric vehicle. It founded that; there has been a strong correlation between the road dynamics; the geographical landscape of the city and the energy consumption of the vehicle. the developed Addis Ababa drive cycle consumed large energy from the storage system and additionally the nature of the city is very convenient to regenerative braking energy as well. From the finding, this thesis recommends that the adoption of electric vehicles in the city of Addis Ababa/Ethiopia must consider topographic distribution and road dynamics; and further investigation is advisable. Due to the effect of geographical distribution and traffic road dynamics of the city require some unique design approach for electric vehicle energy storage

system. On the other side, due to large input impedance, the ESS incorporate with batteries only is less efficient to capture regenerative energy compared to HESS. It is recommended to use additional high-power density auxiliary energy storage devices in conjunction with batteries. Adopting electric vehicles without considering the above issue may lead to performing within the manufacturers' specifications. Specifically degrade the performance of batteries and reduced the total range of travel per single charge.

5.2 Future work

Here is list of recommendations to the possible extensions of the works of this research:

- Limitation of work
  - Due to the absence of topographic data of international standard drive cycle, the impact of geographical data has been assessed using the maximum limit of road grade by refereeing international standard (ASHEETO) considered. If topographic data of specific city was available, it very important to get accurate and effective representation of result can be found.
  - For simulation work, this thesis implemented the generic built in battery model. For better accuracy of estimation, it is suggested to model the battery packs. this could effectively analyze the impact due to temperature effect. In addition, that accurate state of charge estimation can be found.
  - In the vehicle model, only the propulsion load of the vehicle was considered. This can be improved considering additional non population load model.
- Any interested person who wants to study further may accomplished the remaining works:
  - Due to the absence of topographic data of international standard drive cycle, the impact of geographical data has been assessed using the maximum limit of road grade by refereeing international standard (ASHEETO) considered. In order to identify the exact impact of road grade, a more advanced and accurate date must be found. This can be found collaboration between different stakeholders. So that, the researcher should address this issue.
  - The impact of atmospheric temperature of Addis Ababa city and the corresponding internal temperature of battery packs should be considered in future work. This will help to analyze the effect of internal temperature variation on battery packs.
  - Due to temperature sensitive behavior of batteries cell voltage equalization must be considered in future design.

References

[1] FDRE, “Climate Resilient Green Economy (CRGE)” Addis Ababa/ Ethiopia pp 1-200, 2010.

[2] Yamanaka, M.; Ikuta, K.; Matsui, T.; Nakashima, H.; Tomokuni, Y.; "A life indicator of stationary type sealed lead-acid battery," Telecommunications Energy Conference, 1991. INTELEC '91., 13th International, vol., no., pp.202-208, 5-8 Nov 1991

[3] N. Watrin, B. Blunier, and A. Miraoui, “Review of adaptive systems for lithium batteries state-of-charge and state-of-health estimation,” in Proceedings of IEEE Transportation Electrification Conference and Expo, pp. 1–6, Dearborn, Mich, USA, June 2012. View at Publisher · View at Google Scholar

[4] S. Piller, M. Perrin, and A. Jossen, “Methods for state-of-charge determination and their applications,” Journal of power sources, vol. 96, no. 1, pp. 113–120, 2001.

[5] K. S. Ng, C. S. Moo, Y. P. Chen, and Y. C. Hsieh, “Enhanced coulomb counting method for estimating state-of-charge and state-of-health of lithium-ion batteries,” Applied Energy, vol. 86, no. 9, pp. 1506–1511, 2009.

[6] Yinjiao Xing, Wei He b, Michael Pecht b, Kwok Leung Tsui “State of charge estimation of lithium-ion batteries using the open-circuit voltage at various ambient temperatures” A Department of Systems Engineering and Engineering Management, City University of Hong Kong, 83 Tat Chee Avenue, Kowloon, Hong Kong B. Centre for Advanced Life Cycle Engineering (CALCE), University of Maryland, College Park, MD 20740, USA

[7] P. Singh, C. Fennie, D. Reisner, and A. Salkind, “A fuzzy logic approach to state-of-charge determination in high performance batteries with applications to electric vehicles,” in 15th Electric Vehicle Symposium, vol. 15, 1998, pp. 30–35.

[8] G. Ren, G. Ma, and N. Cong, “Review of electrical energy storage system for vehicular applications,” Renewable and Sustainable Energy Reviews, vol. 41, pp. 225–236, 2015.

[9] Sh. Lu, K.A. Corzine, M. Ferdowsi, IEEE Trans. Veh. Technol. 56 (2007) 1516.

[11] N. Schofield, H. T. Yap, and C. M. Bingham, "Hybrid energy sources for electric and fuel cell vehicle propulsion," presented at IEEE Vehicle Power and Propulsion Conference, VPPC,2005.

[12] Cheng H, et al. Demonstration of ultra-high recyclable energy densities in domain-engineered ferro-electric films. Nat Commun 2017;8:1999.

[13] M. Endo, T. Takeda, Y. J. Kim, K. Koshiba, and K. Ishii, "High Power Electric Double Layer Capacitor (EDLCes) from Operating Principle to Pore Size Control in Advanced

Activated Carbons," Carbon Science, vol. 1, pp. 117-128, 2001.

[14] A. Rufer, P. Barrade, D. Hotellier, and P. Derron, "Supercapacitive energy storage: Power electronic solutions and applications," presented at Associazione Nazionale Azionamenti Elettrici, 13o Seminario Interattivo, Azionamenti elettrici: Evoluzione Tecnologica e Problematiche Emergenti, Bressanone, Italy. source: http://leiwww.epfl.ch, 2002.

[15] P. Barrade and A. Rufer, "The use of super capacitors for energy storage traction systems," presented at IEEE Vehicle Power and Propulsion Conference, 2004.

[16] R. A. Dougal, S. Liu, and R. E.White, "Power and Life Extension of Battery - Ultra capacitor-Hybrids," IEEE Transactions on Components and Packaging Technologies, [see also, IEEE Transactions on Components, Packaging and Manufacturing Technology, Part A: Packaging Technologies]", vol. 25, pp. 120-131, 2002.

[17] F. Gagliardi and M. Pagano, "Experimental Results of on-board Battery-Ultra capacitor System for Electric Vehicle Applications," presented at Proceedings of the 2002 IEEE International Symposium on Industrial Electronics, 2002.

[18] Mazen Yassine and Drazen Fabris, "Performance of Commercially Available Super capacitors" Mechanical Engineering Department, Santa Clara University, Santa Clara, CA 95053, USA, Published: 5 September 2017

[19] E. Ozatay, B. Zile, J. Anstrom, and S. Brennan., "Power distribution control coordinating ultra-capacitors and batteries for electric vehicles," presented at Proceedings of the American Control Conference, 2004. [20, 21 & 22].

[20] Khaligh, Alireza, and Zhihao Li. "Battery, ultracapacitor, fuel cell, and hybrid energy storage systems for electric, hybrid electric, fuel cell, and plug-in hybrid electric vehicles: State of the art." IEEE transactions on Vehicular Technology 59.6 (2010): 2806-2814.

[21] Puşcaş, A. M., et al. "Thermal and voltage testing and characterization of super capacitors and batteries." Optimization of Electrical and Electronic Equipment (OPTIM), 2010 12th International Conference on. IEEE, 2010.

[22] Hossain, Shaik Asif, Monir Hossen, and Shamim Anower. "ESTIMATION OF DAMSELFISH BIOMASS USING AN ACOUSTIC SIGNAL PROCESSING TECHNIQUE." Journal of Ocean Technology 13.2 (2018).

[23] He, H.W; Xiong, R.; Chang, Y.H. Dynamic Modeling and Simulation on a Hybrid Power System for Electric Vehicle Applications. Energies 2010, 3, 1821–1830.

[24] Michalczuk, M., L. M. Grzesiak, and B. Ufnalski. "Hybridization of the lithium energy storage for an urban electric vehicle." Bulletin of the Polish Academy of Sciences: Technical Sciences 61.2 (2013): 325-333.

[25] X. Yan and D. Patterson, "Improvement of Drive Range, Acceleration and Deceleration Performance in an Electric Vehicle Propulsion System," presented at 30th Annual IEEE Power Electronics Specialists Conference, 1999.

[26] L. Gao, R. A. Dougal, and S. Liu, "Power enhancement of an actively controlled battery/ ultra-capacitor hybrid," IEEE Transactions on Power Electronics, vol. 20, pp. 236-243, 2005.

[27] L. Gao, R. A. Dougal, and S. Liu, "Active Power Sharing in Hybrid Battery/Capacitor Power Sources," presented at Applied Power Electronics Conference and Exposition, APEC '03, 2003.

[28] A. Kuperman and I. Aharon, “Battery-ultra capacitor hybrids for pulsed current loads: a review,” Renewable and Sustainable Energy Reviews, vol. 15, no. 2, pp. 981–992, 2011.

[29] M. Ortuzar, J. Moreno, and J. Dixon, “ultra-capacitor-based auxiliary energy system for an electric vehicle: implementation and evaluation,” IEEE Transactions on Industrial Electronics, vol. 54, no. 4, pp. 2147–2156, 2007.

[30] G. Steinmauer and L. d. Re, "Optimal control of dual power sources," presented at Proceedings of the IEEE International Conference on Control Applications, CCA '01, 2001.

[31] J. M. Miller, P. J. McCleer, M. Everett, and E. G. Strangers, "Ultra-capacitor Plus Battery Energy Storage System Sizing Methodology for HEV Power Split Electronic CVT's," presented at Proceedings of the IEEE International Symposium on Industrial Electronics, ISIE 2005., 2005

[32] A. Lohner and W. Evers, "Intelligent power management of a super capacitor based hybrid power train for light-rail vehicles and city busses," presented at IEEE Power Electronics Specialists Conference, PESC 04, 2004.

[33] M. J. West, C. M. Bingham, and N. Schofield, "Predictive control for energy management in all/more electric vehicles with multiple energy storage units," presented at IEEE International Electric Machines and Drives Conference, IEMDC'03, 2003.

[34] L. Guzzella and A. Sciarretta, Vehicle Propulsion Systems - Introduction to Modeling and Optimization: Springer, ISBN 3-540-25195-2, 2005.

[35] M. J. Gielniak and J. Z. Shen, "Power management strategy based on game theory for fuel cell hybrid electric vehicles," presented at IEEE Vehicular Technology Conference, VTC Fall, 2004.

[36] H. Y. Tong, W. T. Hung, and C. S. Cheung, “Development of a driving cycle for Hong Kong,” Atmos. Environ., vol. 33, no. 15, pp. 2323–2335, 1999.

[37] G. Amirjamshidi and M. Roorda, “Development of Simulated Driving Cycles: Case study of the Toronto Waterfront Area,” Transp. Res. Board Annu. Meet., vol. 34, no. 227, pp. 255–266, 2013.

[38] A. R. Mahayadin et al., “Efficient methodology of route selection for driving cycle development,” in Journal of Physics: Conference Series, 2017.

[39] Haider S. Najem, Qahtan A. Jawad, Abdulbaki K. Ali, and Basil S. Munahi, “Developing a General Methodology and Construct a Driving Cycle with an Economic Performance Evaluation for Basrah City”, International Journal of Engineering & Technology, 2018

[40] American Association of State Highway and Transportation Officials (AASHTO) standards, road way design manual, 2017

[41] Climatic, environmental and human consequences of the largest known historic eruption: Tambora volcano (Indonesia) 1815. Prog Phys Geogr 27:230–259, Oppenheimer C (2003)

[41] Amirjamshidi, G.; Roorda, M.J. Development of simulated driving cycles for light, medium, and heavy duty trucks: Case of the Toronto Waterfront Area. Transp. Res. Part. D Transp. Environ. 2015, 34, 255–266.

Appendices1. Fuzzy Logic Rules for HESS

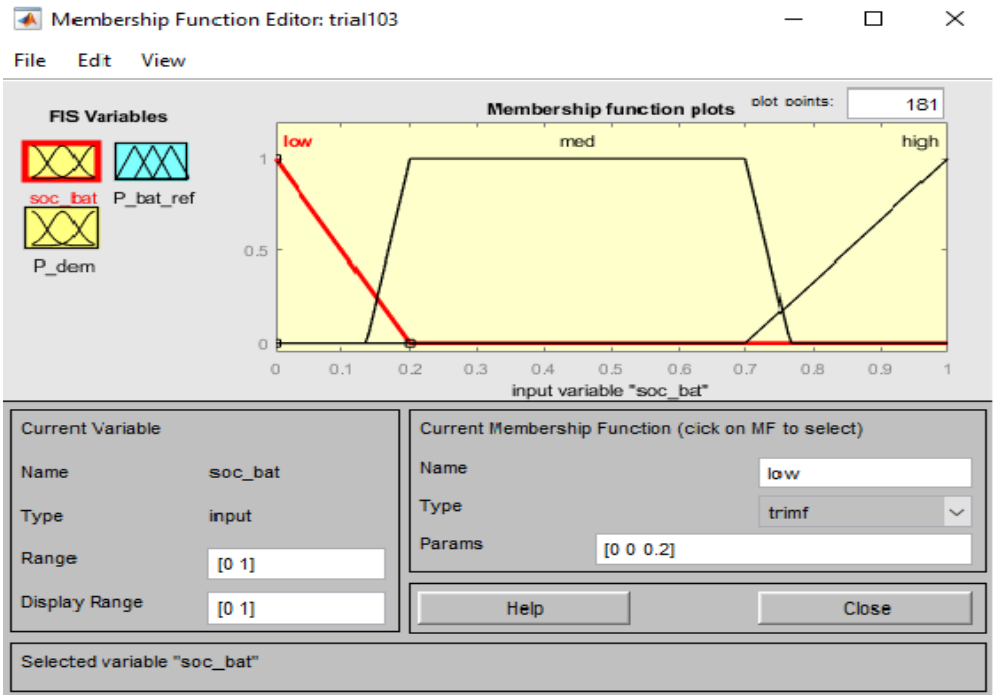

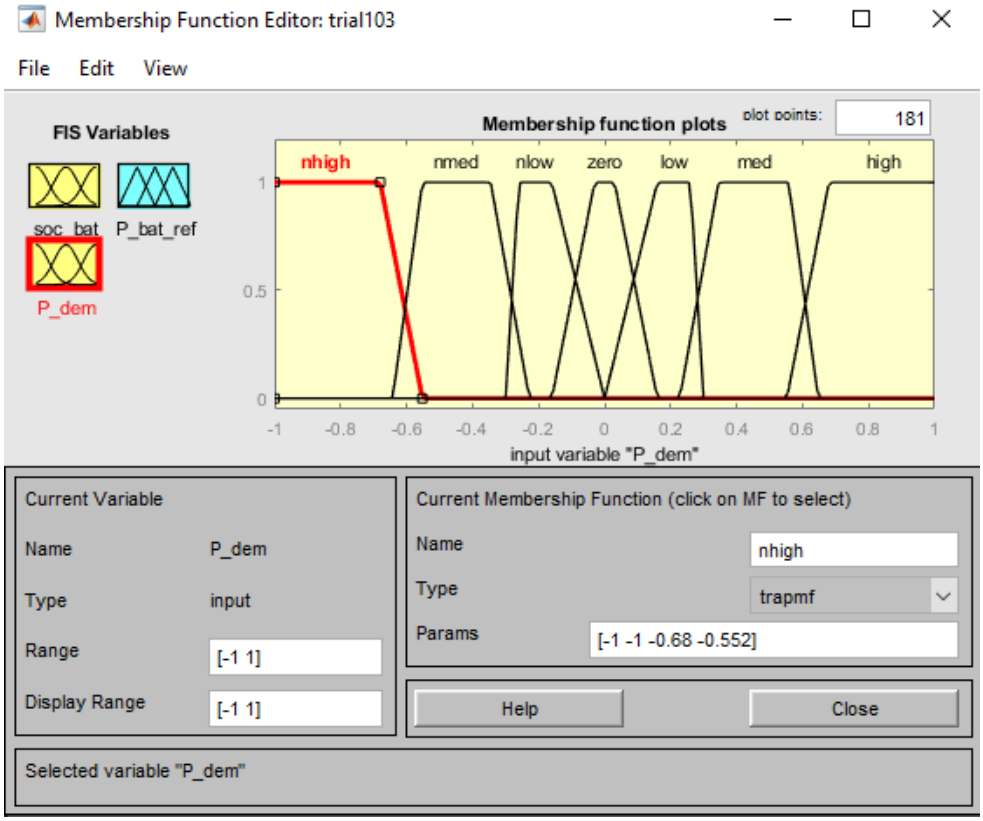

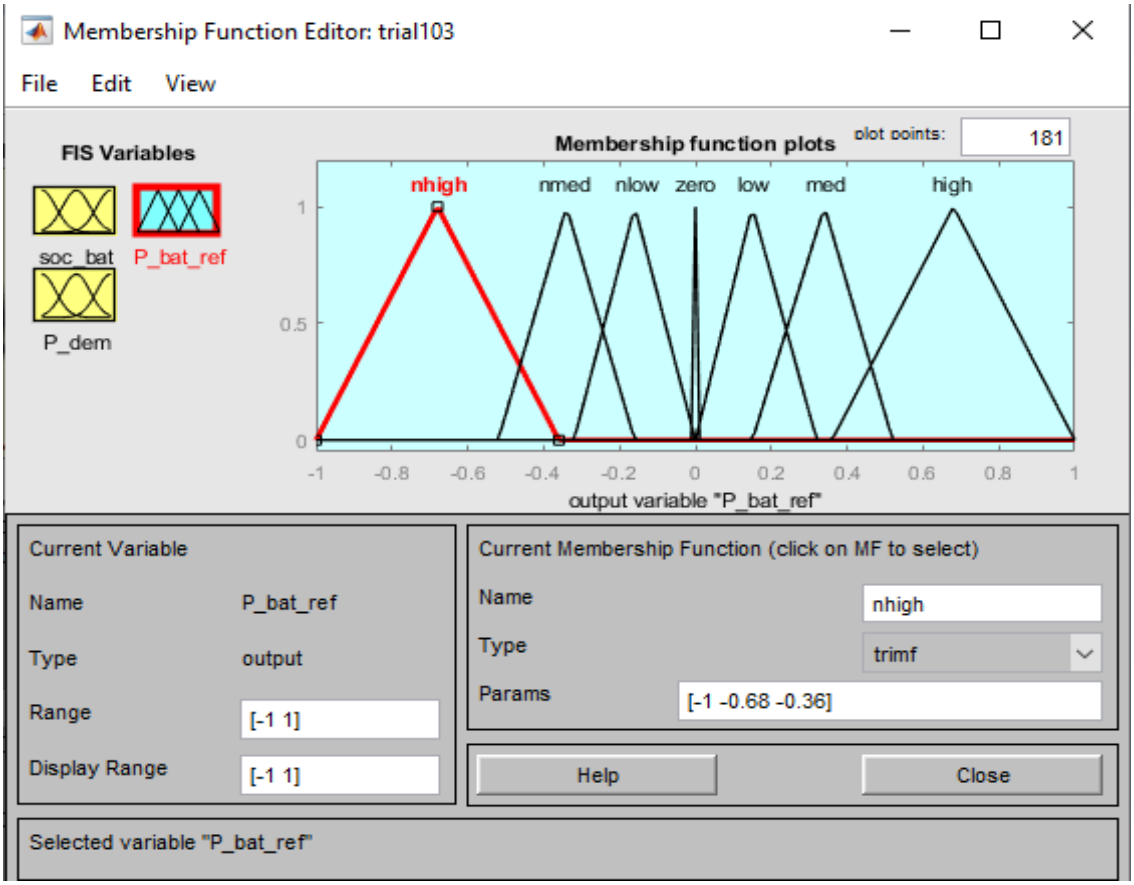
Membership Function Editor: trial103
File Edit View
FIS Variables
soc_bat
P_bat_ref
P_dem
Membership function plots
plot points:
181
nhigh
nmed
nlow
zero
low
med
high
output variable "P_bat_ref"
Current Variable
Name P_bat_ref
Type output
Range [-1 1]
Display Range [-1 1]
Current Membership Function (click on MF to select)
Name nhigh
Type trimf
Params [-1 -0.68 -0.36]
Help
Close
Selected variable "P_bat_ref"

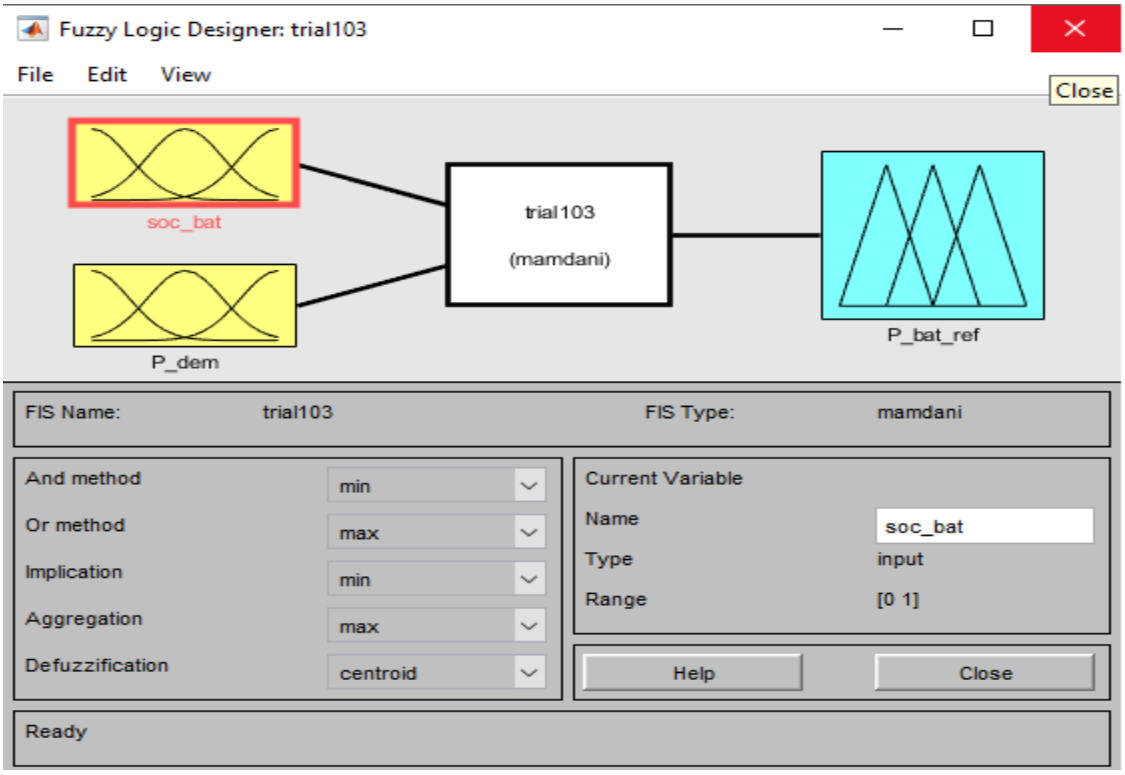
Fuzzy Logic Designer: trial103
File Edit View
Close
soc_bat
P_dem
trial103
(mamdani)
P_bat_ref
FIS Name: trial103
FIS Type: mamdani
And method min
Or method max
Implication min
Aggregation max
Defuzzification centroid
Current Variable
Name soc_bat
Type input
Range [0 1]
Help
Close
Ready

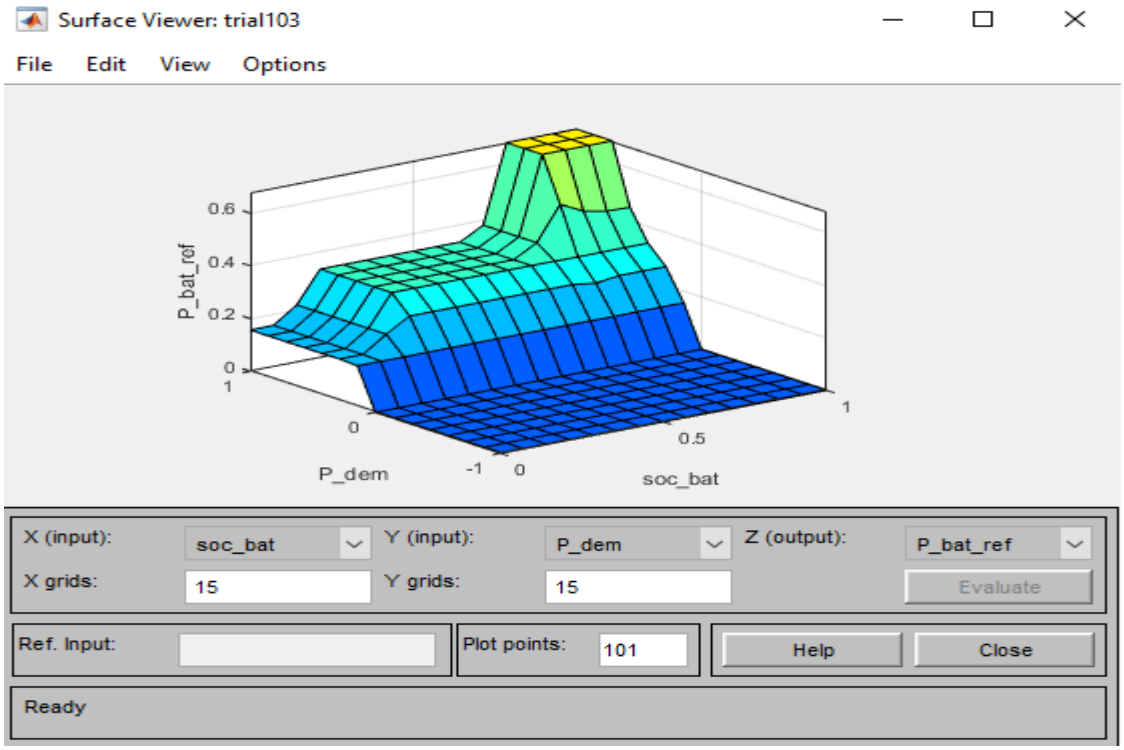
Surface Viewer: trial103
File Edit View Options
P_bat_ref
0.6
0.4
0.2
0
1
0
-1
P_dem
0
0.5
1
soc_bat
X (input): soc_bat
Y (input): P_dem
Z (output): P_bat_ref
X grids: 15
Y grids: 15
Evaluate
Ref. Input:
Plot points: 101
Help
Close
Ready

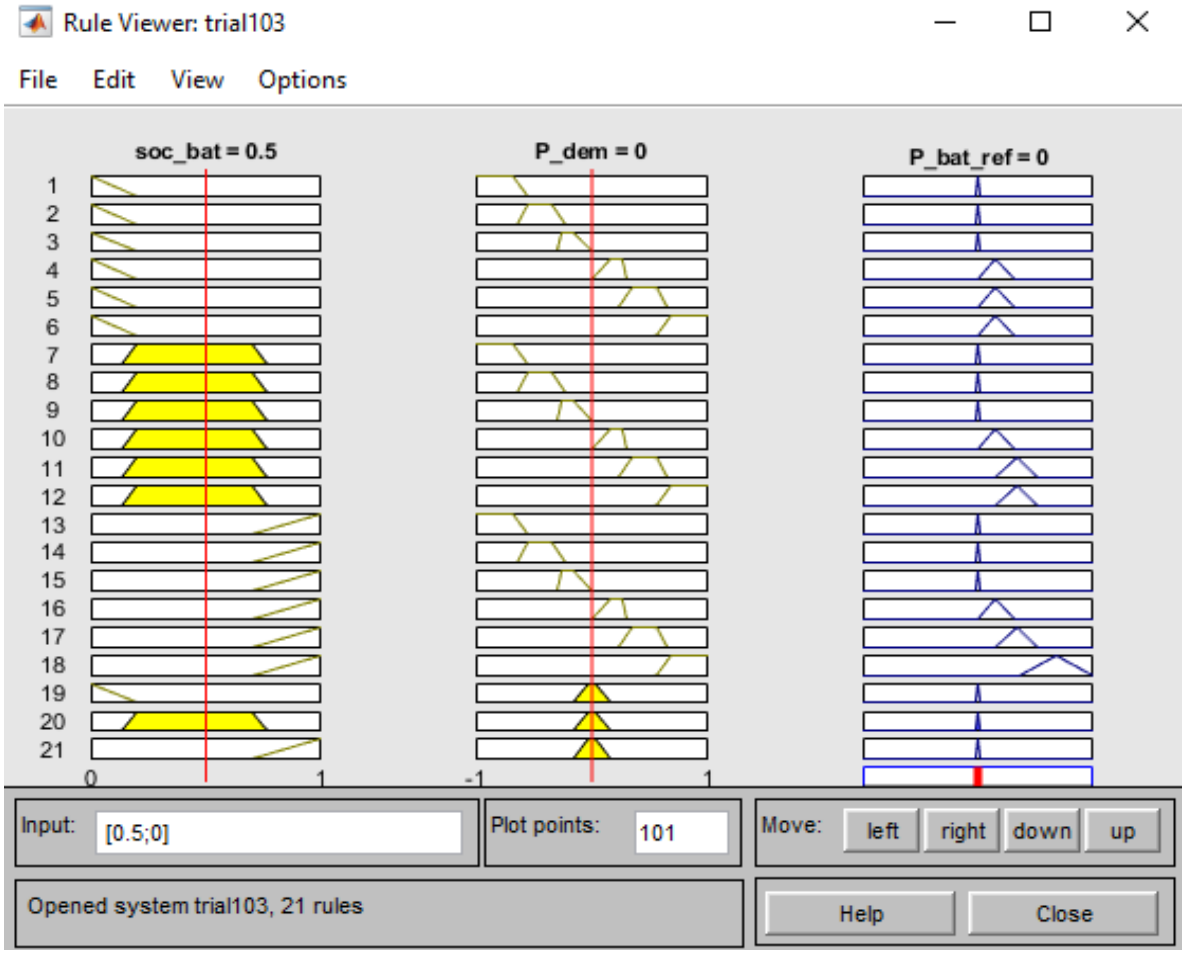
Rule Viewer: trial103
File Edit View Options
soc_bat = 0.5
P_dem = 0
P_bat_ref = 0
1
2
3
4
5
6
7
8
9
10
11
12
13
14
15
16
17
18
19
20
21
0
1
-1
1
Input: [0.5;0]
Plot points: 101
Move: left right down up
Opened system trial103, 21 rules
Help
Close

Fuzzy logic Rules for HESS

1. If (soc_bat is low) and (P_dem is nhigh) then (P_bat_ref is zero) (1)

2. If (soc_bat is low) and (P_dem is nmed) then (P_bat_ref is zero) (1)

3. If (soc_bat is low) and (P_dem is nlow) then (P_bat_ref is zero) (1)

4. If (soc_bat is low) and (P_dem is low) then (P_bat_ref is low) (1)

5. If (soc_bat is low) and (P_dem is med) then (P_bat_ref is low) (1)

6. If (soc_bat is low) and (P_dem is high) then (P_bat_ref is low) (1)

7. If (soc_bat is med) and (P_dem is nhigh) then (P_bat_ref is zero) (1)

8. If (soc_bat is med) and (P_dem is nmed) then (P_bat_ref is zero) (1)

9. If (soc_bat is med) and (P_dem is nlow) then (P_bat_ref is zero) (1)

10. If (soc_bat is med) and (P_dem is low) then (P_bat_ref is low) (1)

11. If (soc_bat is med) and (P_dem is med) then (P_bat_ref is med) (1)

12. If (soc_bat is med) and (P_dem is high) then (P_bat_ref is med) (1)

13. If (soc_bat is high) and (P_dem is nhigh) then (P_bat_ref is zero) (1)

14. If (soc_bat is high) and (P_dem is nmed) then (P_bat_ref is zero) (1)

15. If (soc_bat is high) and (P_dem is nlow) then (P_bat_ref is zero) (1)

16. If (soc_bat is high) and (P_dem is low) then (P_bat_ref is low) (1)

17. If (soc_bat is high) and (P_dem is med) then (P_bat_ref is med) (1)

18. If (soc_bat is high) and (P_dem is high) then (P_bat_ref is high) (1)

19. If (soc_bat is low) and (P_dem is zero) then (P_bat_ref is zero) (1)

20. If (soc_bat is med) and (P_dem is zero) then (P_bat_ref is zero) (1)

21. If (soc_bat is high) and (P_dem is zero) then (P_bat_ref is zero) (1)

Appendices 2. Fuzzy Logic Rules for BESS

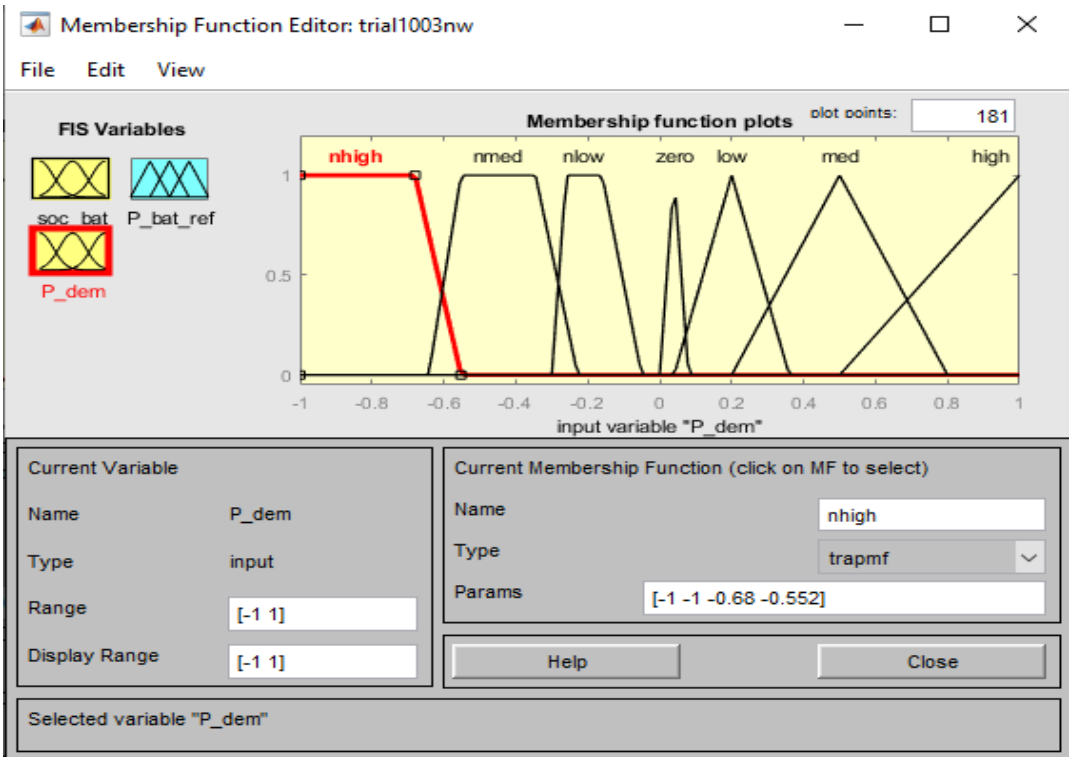

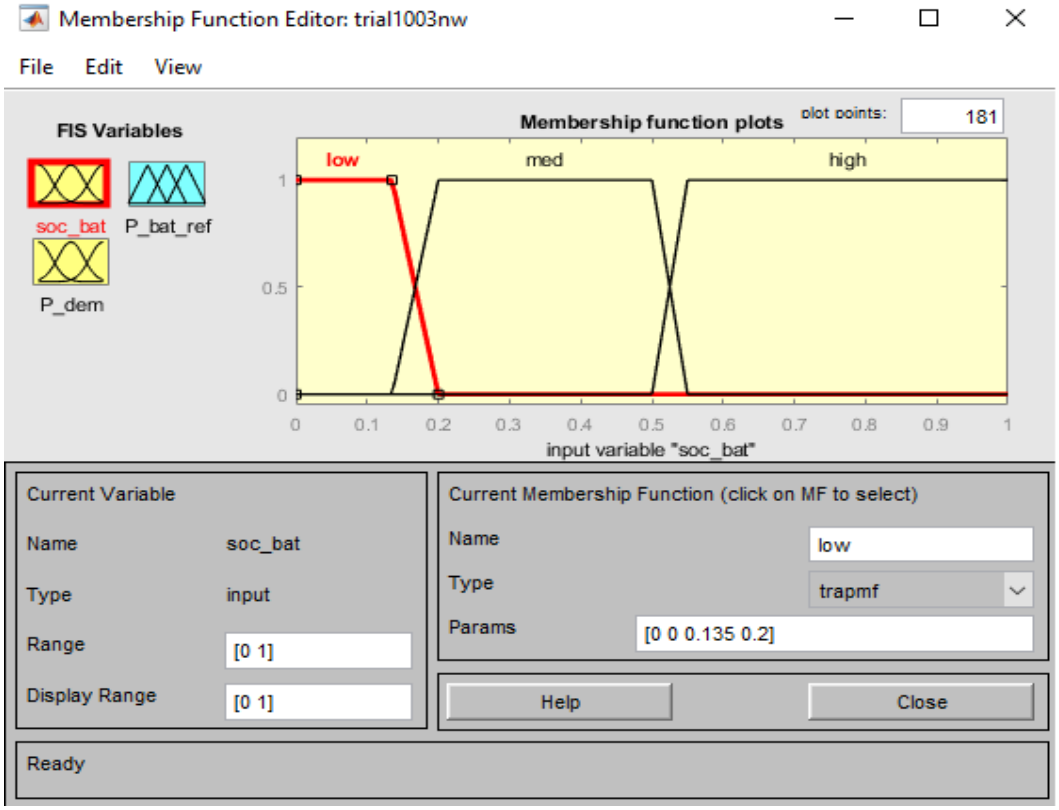

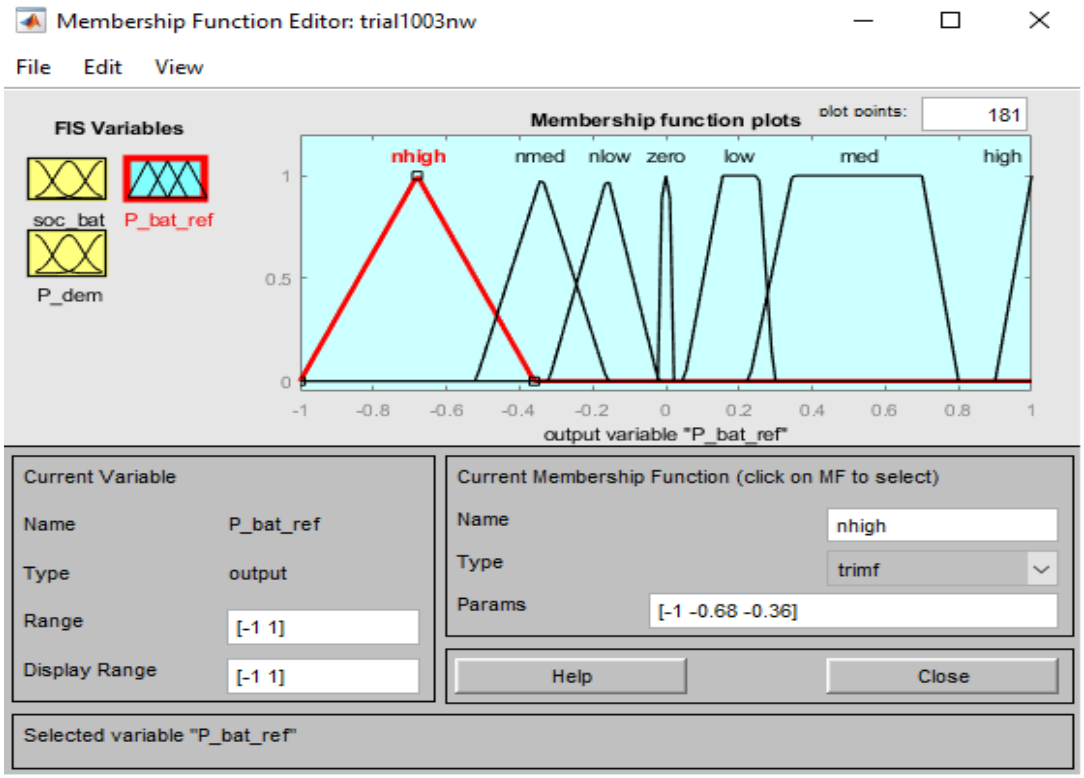
Membership Function Editor: trial1003nw
File Edit View
FIS Variables
soc_bat
P_bat_ref
P_dem
Membership function plots
plot points:
181
nhigh
nmed
nlow
zero
low
med
high
output variable "P_bat_ref"
Current Variable
Name P_bat_ref
Type output
Range [-1 1]
Display Range [-1 1]
Current Membership Function (click on MF to select)
Name nhigh
Type trimf
Params [-1 -0.68 -0.36]
Help
Close
Selected variable "P_bat_ref"

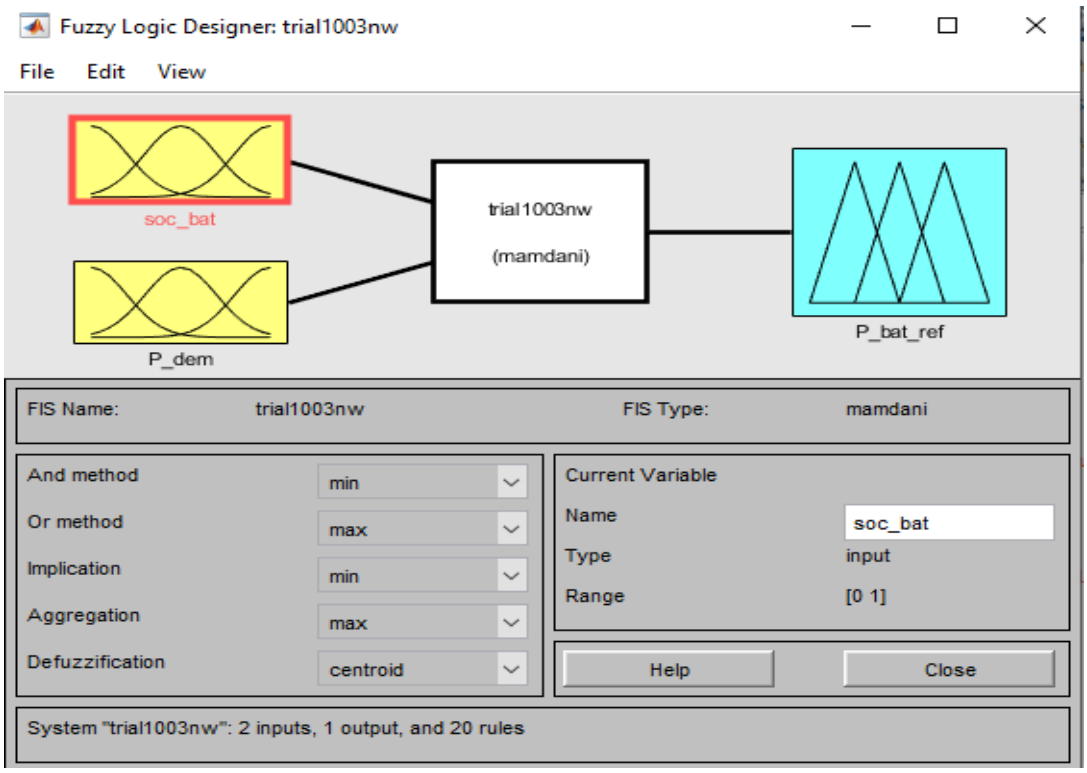
Fuzzy Logic Designer: trial1003nw
File Edit View
soc_bat
P_dem
trial1003nw
(mamdani)
P_bat_ref
FIS Name: trial1003nw
FIS Type: mamdani
And method min
Or method max
Implication min
Aggregation max
Defuzzification centroid
Current Variable
Name soc_bat
Type input
Range [0 1]
Help
Close
System "trial1003nw": 2 inputs, 1 output, and 20 rules

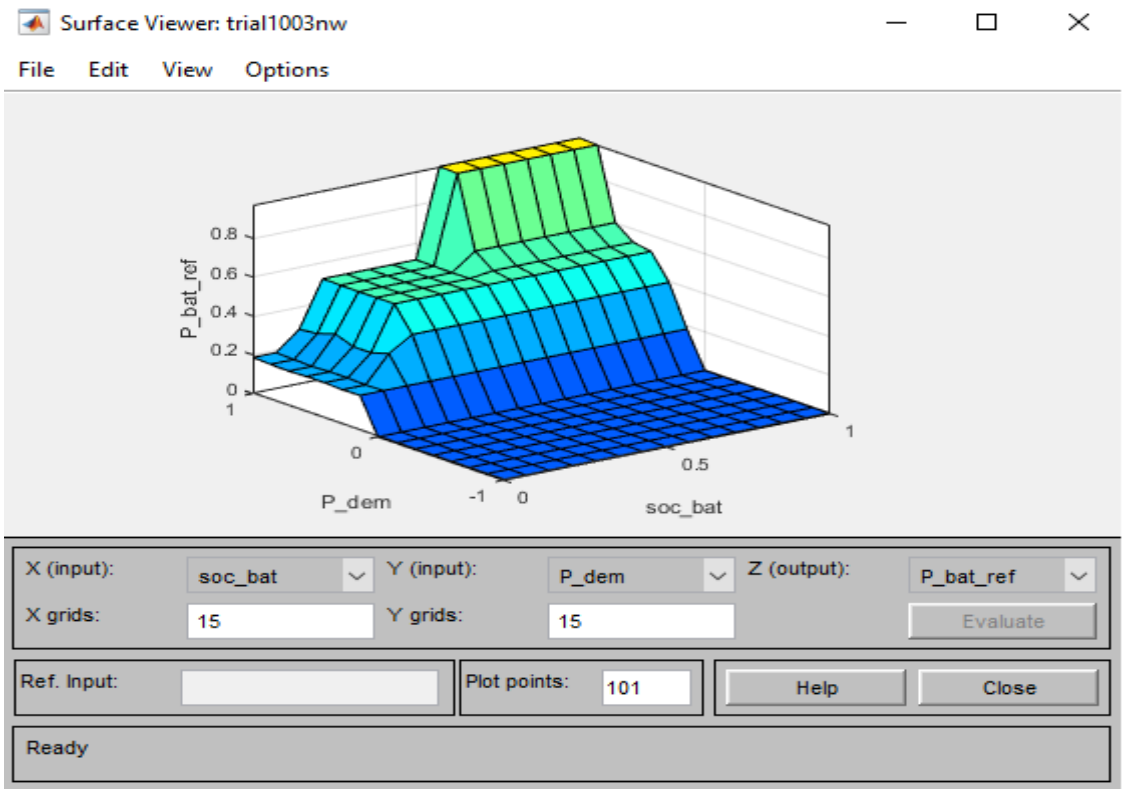
Surface Viewer: trial1003nw
File Edit View Options
P_bat_ref
0.8
0.6
0.4
0.2
0
1
0
-1
P_dem
0
0.5
1
soc_bat
X (input): soc_bat
Y (input): P_dem
Z (output): P_bat_ref
X grids: 15
Y grids: 15
Evaluate
Ref. Input:
Plot points: 101
Help
Close
Ready

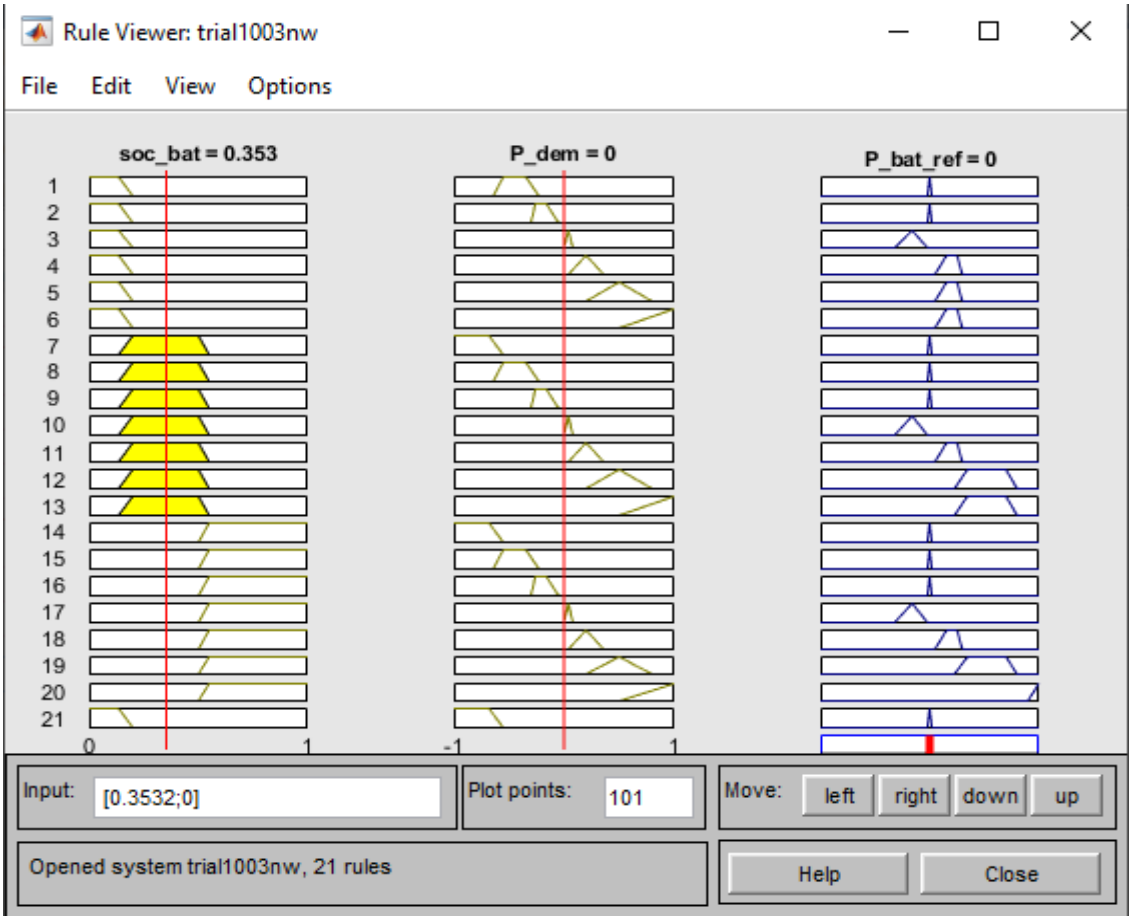
Rule Viewer: trial1003nw
File Edit View Options
soc_bat = 0.353
P_dem = 0
P_bat_ref = 0
1
2
3
4
5
6
7
8
9
10
11
12
13
14
15
16
17
18
19
20
21
0
1
-1
1
Input: [0.3532;0]
Plot points: 101
Move: left right down up
Opened system trial1003nw, 21 rules
Help
Close

Fuzzy logic Rules for BESS

1. If (soc_bat is low) and (P_dem is nmed) then (P_bat_ref is zero) (1)
2. If (soc_bat is low) and (P_dem is nlow) then (P_bat_ref is zero) (1)
3. If (soc_bat is low) and (P_dem is zero) then (P_bat_ref is nlow) (1)
4. If (soc_bat is low) and (P_dem is low) then (P_bat_ref is low) (1)
5. If (soc_bat is low) and (P_dem is med) then (P_bat_ref is low) (1)
6. If (soc_bat is low) and (P_dem is high) then (P_bat_ref is low) (1)
7. If (soc_bat is med) and (P_dem is nhigh) then (P_bat_ref is zero) (1)
8. If (soc_bat is med) and (P_dem is nmed) then (P_bat_ref is zero) (1)
9. If (soc_bat is med) and (P_dem is nlow) then (P_bat_ref is zero) (1)
10. If (soc_bat is med) and (P_dem is zero) then (P_bat_ref is nlow) (1)
11. If (soc_bat is med) and (P_dem is low) then (P_bat_ref is low) (1)
12. If (soc_bat is med) and (P_dem is med) then (P_bat_ref is med) (1)
13. If (soc_bat is med) and (P_dem is high) then (P_bat_ref is med) (1)
14. If (soc_bat is high) and (P_dem is nhigh) then (P_bat_ref is zero) (1)
15. If (soc_bat is high) and (P_dem is nmed) then (P_bat_ref is zero) (1)
16. If (soc_bat is high) and (P_dem is nlow) then (P_bat_ref is zero) (1)
17. If (soc_bat is high) and (P_dem is zero) then (P_bat_ref is nlow) (1)
18. If (soc_bat is high) and (P_dem is low) then (P_bat_ref is low) (1)
19. If (soc_bat is high) and (P_dem is med) then (P_bat_ref is med) (1)
20. If (soc_bat is high) and (P_dem is high) then (P_bat_ref is high) (1)
21. If (soc_bat is low) and (P_dem is nhigh) then (P_bat_ref is zero) (1)

Appendices 3 Parameter Calculations for bi-directional DC-DC convertor

Battery converter calculations

	Parameter	Values
1	Maximum converter requirement	60 KW
2	Battery output voltage range (discharging)	330 -360 V
3	Battery input voltage range (charging)	255 – 330 V
4	DC buss voltage	360 – 400 V
5	Switching frequency	1khz
6	Percentage Battery discharge current ripple	1%
7	Percentage Battery charging current ripple	1%
8	Dc buss voltage variation	2%

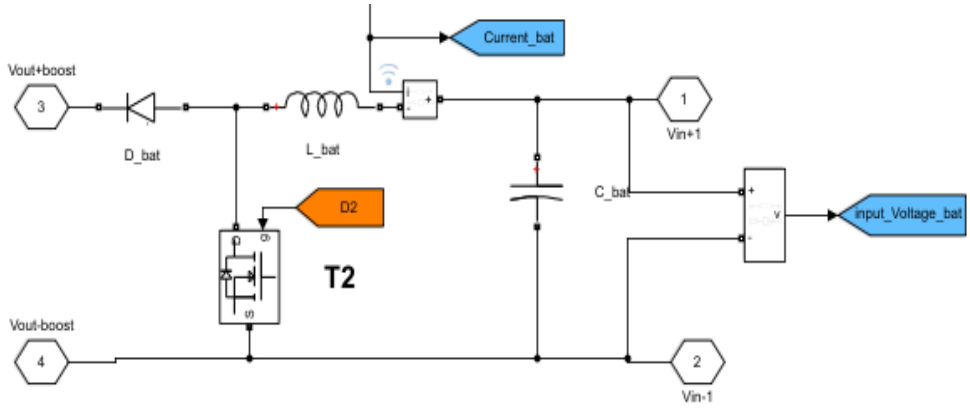

Boost mode

Case 1

DT2 is the duty cycle of the Transistor T2

When Transistor T2 = on

The voltage equation of battery boost circuit became

$$vin - L_{bat}\frac{di_{bat}}{dt_{on}} = 0 \quad \text{..... eq 1.1}$$

$$vin - L\_bat\frac{\Delta\, i\_bat}{DT_2} fsw = 0 \text{ ..... eq 1.2}$$

Rearranging equation 1.2 became

$$vin\,(DT_2) = L_{bat}.\Delta\, i\_bat\,.fsw \text{ ..... eq 1.3}$$

Case 2

When Transistor T2 = off

$$vout - L\_bat\frac{di\_bat}{dt_{off}} - vin = 0 \text{..... eq 1.4}$$

$$vout - L\_bat\frac{\Delta\, i\_bat}{(1-DT_2)}fsw - vin = 0 \text{ ..... eq 1.5}$$

By rearranging equation 1.5 became

$$(vout - vin)(1 - DT_2)\, L_{bat} * \Delta\, i_{bat} * fsw \text{ .....eq 1.6}$$

Equating terms $L_{bat}.* \Delta\, i_{bat} * fsw$ in equation 1.5 and 1.6. and factoring out gives the voltage transfer function as

$$\frac{vout}{vin} = \frac{1}{(1-DT_2)} \text{ ..... eq 1.7}$$

When the SOC of the battery is 100%, The battery terminal voltage is at its maximum open-circuit voltage where the unit terminal voltage is 13.2V. For this design, we have used 25 cells connected in series to meet the design voltage specification (330V in series). The duty cycle is minimum at this condition and is calculates as,

$$DT_2\, min = 1 - \frac{Vbat\, max}{vout} \text{.....eq 1.8}$$

$$DT_2\, min = 1 - \frac{330}{380}$$

$$\boldsymbol{DT_2\, min = 0.13}$$

When the SOC of the battery is discharged fully, the unit battery terminal voltage drops to 10.2V and consequently, the overall terminal voltage drops to 255V. The resultant duty cycle is maximum in this condition and is calculated as,

$$DT_2\, max = 1 - \frac{Vbat\, min}{vout} \text{.....eq 1.9}$$

$$DT_2\, max = 1 - \frac{255}{380} \text{.....eq 1.9}$$

$$\boldsymbol{DT_2\, max = 0.32}$$

Therefore, the boost or discharge mode of operation on the battery side considering only the input to output voltage transfer function results in a duty cycle range of $0.13 \leq D \leq 0.328$. For a fixed switching frequency of 1kHz (0.001s period), Transistor T2 will be in conduction for a maximum of

$$T2_{max} = \frac{1}{fsw} DT_2 max \text{ ..... eq 2.0}$$

$$T2_{max} = \frac{1}{1000} * 0.328$$

$$\boldsymbol{T2_{max} = 328\ \mu s}$$

Similarly, Transistor T2 will be in conduction for a minimum of

$$T2_{min} = \frac{1}{fsw} DT_2 min \ldots\ldots\ldots\ldots\ldots\ldots \text{ eq 2.1}$$

$$T2_{max} = \frac{1}{1000} * 0.13$$

$$\boldsymbol{T2_{max} = 130\ \mu s}$$

During the conduction period of T2, the inductor voltage is simply Vbatt.

$$v_{bat} = L\_bat \frac{di\_bat}{dt} = L\_bat \frac{\Delta\, i\_bat}{\Delta\, t} \ldots\ldots\ldots\ldots\ldots\ldots\text{eq 2.2}$$

For this design, assuming current ripple is 1% and a mean current, I_bat_mean of 100A, the total peak-to-peak variation

$$\Delta\, i\_bat = 2(0.01 * i\_bat\_mean) \ldots\ldots\ldots \text{ eq 2.3}$$

$$\Delta\, i\_bat = 2(0.01 * 100)$$

$$\boldsymbol{\Delta\, i\_bat = 2\ A}$$

The inductance required at maximum (V batt_max) is,

$$L\_bat = \frac{(vbat\_\max)(\Delta T_{min})}{\Delta\, i\_bat} \ldots\ldots\ldots \text{ eq 2.4}$$

$$L\_bat = \frac{(330v)(0.00013\ s)}{2}$$

$$\boldsymbol{L\_bat = 21,450\ \mu H}$$

For the same ripple current, the inductance required at minimum (V batt_min) is,

$$L\_bat = \frac{(vbat\_\min)(\Delta T_{max})}{\Delta\, i\_bat} \ldots\ldots\ldots \text{ eq 2.5}$$

$$L\_bat = \frac{(255v)(0.000328\ s)}{2}$$

$$\boldsymbol{L\_bat = 41,820\ \mu H}$$

in order to operate the battery boost converter section within the design specifications large inductance value is chosen therefore, the inductance value of 41,820 µH is chosen

The DC bus voltage VDC, the maximum load current is,

$$Iload_{max} = \frac{pmax}{VDC} \ldots\ldots\ldots\ldots\ldots\ldots\text{eq 2.6}$$

$$I\_bat\_load_{max} = \frac{58kw}{380v}$$

$$I\_bat\_load_{max} = 152\ A$$

For a DC bus voltage variation from nominal of 2%.

$$\Delta \boldsymbol{VDC} = 2\%\ vout \quad \text{..... Eq 2.7}$$

$$\Delta \boldsymbol{VDC} = 2\%\ vout$$

$$\Delta \boldsymbol{VDC} = 7.2\text{V}$$

$$Cdc_{min} = \frac{(icdc_{max})(\Delta tmax)}{\Delta \boldsymbol{VDC}} \quad \text{..... eq 2.8}$$

$$Cdc_{min} = \frac{160 * 328\mu \boldsymbol{s}}{7.2\ v}$$

$$= \mathbf{7288.8\ \mu F}$$

Ultra-capacitor side converter calculations

	Parameter	Values
1	Maximum converter requirement	25 KW
2	Ultra-capacitor input voltage range (charging)	162 – 332 V
3	DC buss voltage	360 – 400 V
4	Switching frequency	1khz
5	Percentage Ultra-capacitor discharging current ripple	2%
6	Percentage Ultra-capacitor charging current ripple	2%
7	Dc buss voltage variation	2%

Boost mode

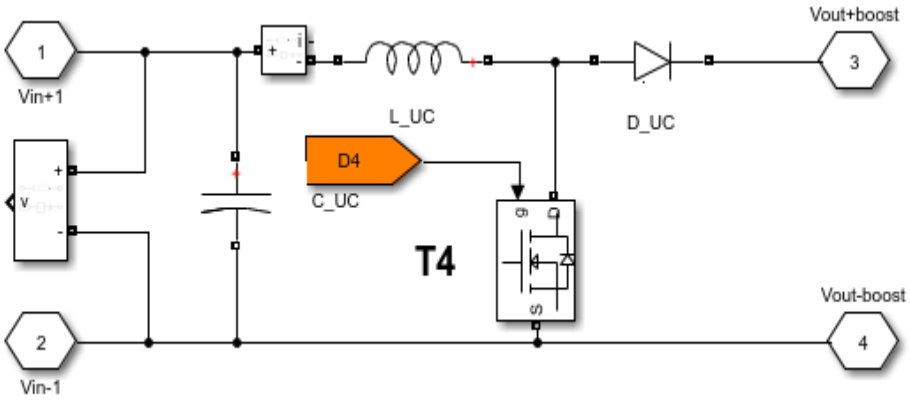

Case 1 and Case 2

DT4 is the duty cycle of the Transistor T4

T4 = on

T4 = off

For the ultra-capacitor section in boost operation mode, the derivations transfer function of converter is similar to battery side converter except for voltage level variation. In this design, we have used 58F/333V ultra-capacitor pack for simulation purposes. Therefore, ultra-capacitor operating voltage ranges from 162V ≤ VUC ≤ 330V. Transistor T4 is modulated to control the ultra-capacitor power flow in discharge mode. Since the derivation is similar to boost mode of battery, the output to input voltage transfer function is

$$\frac{vout}{vin} = \frac{1}{(1-DT_4)} \quad \text{..... eq 2.9}$$

When the SOC of the ultra-capacitor is 100%, The terminal voltage is at its maximum open-circuit voltage where the unit terminal voltage is 2.77V. For this design, we have been used 120 cells connected in series to meet the design voltage specification (332V in series). The duty cycle is minimum at this condition and is calculates as,

$$DT_4\,min = 1 - \frac{V\_uc\_max}{vout} \quad \text{.....eq 3.0}$$

$$DT_4\,min = 1 - \frac{332}{380}$$

$$\boldsymbol{DT_4\,min = 0.126}$$

When the SOC of the ultra-capacitor is discharged fully, the unit terminal voltage drops to 1.35V and consequently, the overall terminal voltage drops to 162V. The resultant duty cycle is maximum in this condition and is calculated as,

$$DT_4\,max = 1 - \frac{V\_uc\_max}{vout} \quad \text{.....eq 3.1}$$

$$DT_4\,max = 1 - \frac{162}{380} \quad \text{.....eq 3.2}$$

$$\boldsymbol{DT_4\,max = 0.573}$$

Therefore, the boost or discharge mode of operation on the ultra-capacitor side considering only the input to output voltage transfer function results in a duty cycle range of 0.126 ≤ D ≤ 0.573. For a fixed switching frequency of 1kHz (0.001s period), Transistor T4 will be in conduction for a maximum of

$$T4_{max} = \frac{1}{fsw} DT_4max \text{ ..... eq 3.3}$$

$$T4_{max} = \frac{1}{1000} * 0.573$$

$$\boldsymbol{T4_{max} = 573\ \mu s}$$

Similarly, Transistor T4 will be in conduction for a minimum of

$$T4_{min} = \frac{1}{fsw} DT_4min \text{ ..... eq 3.4}$$

$$T4_{max} = \frac{1}{1000} * 0.126$$

$$\boldsymbol{T4_{max} = 126\ \mu s}$$

During the conduction period of T4, the inductor voltage is simply V_uc.

$$v_{\_uc} = L\_uc \frac{di_{uc}}{dt} = L\_uc \frac{\Delta\, i\_uc}{\Delta\, t} \text{ .....eq 3.5}$$

For this design, assuming current ripple is 2% and a mean current, I_uc_mean of 50A, the total peak-to-peak variation

$$\Delta\, i\_uc = 2(0.02 * i\_uc\_mean) \text{ ..... eq 3.6}$$

$$\Delta\, i\_uc = 2(0.02 * 50)$$

$$\boldsymbol{\Delta\, i\_uc = 2\ A}$$

The inductance required at maximum V_uc is,

$$L\_uc = \frac{(V\_uc\_max)(\Delta T_{min})}{\Delta\, i\_uc} \text{ ..... eq 3.7}$$

$$L\_uc = \frac{(332v)(0.000126\ s)}{2}$$

$$\boldsymbol{L\_uc = 20,916\ \mu H}$$

For the same ripple current, the inductance required at minimum (V_uc_min) is,

$$L\_uc = \frac{(V\_uc\_min)(\Delta T_{max})}{\Delta\, i\_uc} \text{ ..... eq 3.8}$$

$$L\_uc = \frac{(162v)(0.000573\ s)}{2}$$

$$\boldsymbol{L\_uc = 46,413\ \mu H}$$

in order to operate the ultra-capacitor boost converter section within the design specifications large inductance value is chosen therefore, the inductance value of 46,413 µH is chosen

Buck mode

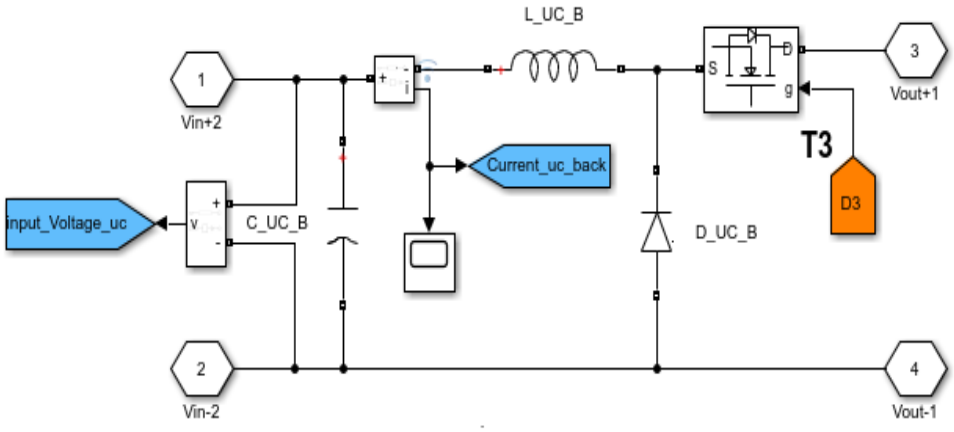

Case 1

When Transistor T3 = on

In the buck mode, the DC Bus voltage acts as the input voltage (Vin), and the ultra-capacitor voltage is the output voltage (Vout) of the converter. Transistor T3 is a key for controlling the buck convertor. the duty cycle of T3 is represented by DT3 with a fixed switching frequency, FSW the voltage equation of ultra-capacitor buck circuit became

$$vin - vout - L\_uc\_B \frac{di\_uc\_B}{dt_{on}} = 0 \quad \text{..... eq 3.9}$$

$$vin - vout - L\_uc\_B \frac{\Delta\, i\_uc\_B}{DT_3} fsw = 0 \quad \text{..... eq 4.0}$$

Rearranging equation 1.2 became

$$(vin - vout)(DT_3) = L_{uc_B} * \Delta\, i_{uc_B} * \ fsw \quad \text{..... eq 4.1}$$

Case 2

When Transistor T3 = off

The KVL loop equation became

$$vout - L\_uc\_B \frac{di\_uc\_B}{dt_{off}} = 0 \text{..... eq 4.2}$$

$$vout - L\_uc\_B \frac{\Delta\, i\_uc\_B}{(1-DT3)} fsw = 0 \text{ ..... eq 4.3}$$

By rearranging equation

$$(vout)(1 - DT_3)\, L_{uc_B} * \ \Delta\, i\_uc\_B\, .fsw \quad \text{.....eq 4.4}$$

Equating terms $L.\Delta i\,.fsw$ in equation 4.3 and 4.4. and factoring out gives the voltage transfer function as

$$\frac{\boldsymbol{vout}}{\boldsymbol{vin}} = \boldsymbol{DT_3} \text{ .....eq 4.5}$$

The DC Bus voltage (VDC) to the buck converter section varies from 360V to 400V by design constrain. When the SOC of the Ultra-capacitor is 100%, The terminal voltage is at its maximum open-circuit voltage where the unit terminal voltage is 2.77 V. For this design, we have used 120 cells connected in series to meet the design voltage specification (332V in series). The minimum threshold voltage where the unit terminal voltage became 1.35V (162V).

$$DT_3\,min = \frac{Vout}{Vin} \text{ .....eq 4.6}$$

$$DT_3\,min = \frac{162}{400}$$

$$\boldsymbol{DT_3\,min = 0.405}$$

When the SOC of the ultra-capacitor is discharged fully, the unit terminal voltage drops to 1.35V and consequently, the overall terminal voltage drops to 162V. The maximum duty cycle occurs when Vin is minimum and Vout is maximum as,

$$DT_3\,max = \frac{Vout}{Vin} \text{ .....eq 4.7}$$

$$DT_3\,max = \frac{332}{360}$$

$$\boldsymbol{DT_3\,max = 0.916}$$

Therefore, the buck or charging mode of operation on the ultra-capacitor side considering only the input to output voltage transfer function results in a duty cycle range of $0.405 \leq D \leq 0.916$. Assuming current ripple is 2% and a mean current, I_uc_mean of 50A, the total peak-to-peak variation

$$\Delta\, i\_uc\_B = 2(0.02 * i\_uc\_mean) \text{ ..... eq 4.8}$$

$$\Delta\, i\_uc\_B = 2(0.02 * 50)$$

$$\boldsymbol{\Delta\, i\_uc\_B = 2\,A}$$

The inductance required at maximum (V_uc_B_max) is,

$$L\_uc\_B = \frac{(Vout)(1-DT_3)}{(\Delta\, i\_uc\_B)fsw} \text{ ..... eq 4.9}$$

$$L\_uc\_B = \frac{(162v)(1-0.405)}{2A*1000hz}$$

$$\boldsymbol{L\_uc\_B = 48,195\ \mu H}$$

For the same ripple current, the inductance required at minimum (V_uc_B_min) is,

$$L\_uc\_B = \frac{(V_{out}\max)(1-DT_3)}{(\Delta i\_uc\_B\ )fsw} \quad \text{..... eq 5.0}$$

$$L\_uc\_B = \frac{(332v)(1-0.916)}{2A*1000hz}$$

$$L\_uc\_B = \boldsymbol{13,944\ \mu H}$$

To operate the ultra-capacitor boost converter section within the design specifications large inductance value is chosen therefore, the inductance value of 46,413 µH is chosen. And assuming voltage ripple 250mv, the required minimum capacitance for the ultra-capacitor buck converter is,

$$C\_Uc\_B_{\_min} = \frac{(V_{out})(1-DT_3)}{L*(\Delta\, Vout)*8(fsw)^2} \quad \text{..... eq 5.1}$$

$$\mathrm{C\_Uc\_B_{\_min}} = \frac{(162)(1-0.405)}{48{,}195*(0.25)*8(1000)^2}$$

$$\boldsymbol{C\_Uc\_B_{\_min} = 1000\mu F}$$

Final Inductive and Capacitive Parameter Values

	Parameter	Mode	Selected Values	Symbol
1	Minimum Ultra-capacitor side inductance	boost	46,413	µH
		buck	48,195	
2	Minimum Ultra-capacitor side input Capacitance	-	1000	µF
3	Minimum Battery side inductance	boost	41,820	µH
		buck	50,000	
4	Minimum Battery side input Capacitance	-	1000	µF
5	Minimum DC buss Capacitance	-	7288	µF

Appendices 4 Road Grade Data for Selected Routes

	Distance travel	Time taken		Initial postion			Final Postion		Avargae altitude	Avargae percentile	max alt gain	Max grade %
Sidestkilo to shero meda	1540	175	2469	9.038289782	38.7548458	2543.0	9.052075724	38.75605016	74	6.60	66	8.20
Betemenegest to pm	604	79	2359	9.010571886	38.7571997	2389.0	9.015953001	38.75774878	30	4.96	25	12.00
Sheraton to pm	324.21	55	2369	9.015956732	38.7536238	2394.0	9.017165307	38.75496251	25	12.20	11	13.00
Tederos to Piyasa	498	71	2343	9.015525678	38.7456914	2383	9.020407747	38.74524939	40	3.97	25	10.80
Tederos to Piyasa _2	701.74	123	2387	9.020587922	38.7452608	2432.0	9.026432843	38.74518627	45	6.41	28	11.10
Tekuranbsa street	647	66	2352	9.019162567	38.7523996	2383	9.018738307	38.74749274	31	4.79	78	13.60
Ethio Medicen factory	667	147	2248	8.981994333	38.7196168	2266	8.986943361	38.72165327	18	5.10	45	8.30
Ruwanda street	404	45	2292	8.982243302	38.7700619	2301	8.983496381	38.77330439	9	2.36	55	13.50
Gofa to behrtsegea	360	120	2226	8.956373334	38.7456706	2248.0	8.956481361	38.74861825	22	6.11	29	12.50